Dynamic Variable Speed Limit Control: Design, Analysis and Benefits

FINAL REPORT

METRANS Project 11-14

By

Petros Ioannou (Principal Investigator)
PhD Students
Yun Wang
Afshin Abadi
Vadim Butakov
University of Southern California
Electrical Engineering - Systems, EEB 200B
Los Angeles, CA 90089-2562
July 28, 2012

Disclaimer

The contents of this report reflect the views of the authors, who are responsible for the facts and accuracy of the information presented herein. This document is disseminated under the sponsorship of the Department of Transportation, University Transportation Centers Program, and California Department of Transportation in the interest of information exchange. The U.S. Government and California Department of Transportation assume no liability for the contents or use thereof. The contents do not necessarily reflect the official views or policies of the State of California or the Department of Transportation. This report does not constitute a standard, specification, or regulation.

Table of Contents

List of Figures

Abstract

Variable speed limit (VSL) systems, as one of the freeway control strategies among Intelligent Transportation Systems (ITS), have been studied since 1970s. However, the cases of field implementations are limited, mostly in Europe and the United States. The VSL systems are considered to reduce risk of crashes, to warn drivers of hazardous roadway conditions, to stabilize and smooth traffic flows, to dampen shock waves, to postpone or prevent congestions, and to reduce emissions and fuel consumptions. The safety benefits of using VSL have been reported in several field studies both in Europe and the United States. Currently, the incentive of using VSL has been mainly safety from the application point of view. However, benefits such as improved traffic flow rates, lower travel times, smooth speed and density distribution and possibly lower pollution have been conjectured in literature and in some cases analyzed using mainly macroscopic traffic models. A closer look at these promising results in the literature shows that using the same macroscopic model to design and test raises questions as to whether the simplicity of the models used for evaluation are responsible for these optimistic results given the fact that other studies using microscopic simulations fail to demonstrate improvements on travel times albeit for different VSL strategies. The question whether the VSL strategies or the macroscopic models used to analyze them or both are responsible for the large differences in traffic flow and travel time benefits reported, remains unanswered. Consequently, the problem of what are the most appropriate dynamic VSL controllers and what benefits can be guaranteed in a consistent manner under different traffic flow conditions is an open one.

In this study, the problems of the design, analysis and evaluation of dynamic VSL controllers are addressed. A control engineering approach is followed, where the control strategies are designed based on simplified models (in this case validated macroscopic traffic flow models) but applied and tested on validated microscopic traffic models under different traffic conditions. Three dynamic VSL control designs, a simple virtual metering strategy which is reactive and non-model based, a nonlinear model predictive controller which is proactive and model based, and a proportional speed controller which only needs traffic density/occupancy as inputs, are presented, tested using both macroscopic and microscopic simulation models. Monte Carlo simulations are conducted for 10 different scenarios using an integrated simulation/evalution framework.

Examining the performance measurements summarized from several hundreds simulations runs, the simple PI type controller with less computational burden is not inferior to the more complicated nonlinear MPC which also needs predicted demand and accident information as inputs. Although macroscopic simulations demonstrates that both simple controller and model predictive controller could reduced Total Time Spent (TTS) for about 20%, VISSIM microscopic simulations show that Total Travel Time (TTT) could not be improved by variable speed limit controllers due to the vehicle level transient responses and the second rate shock wave generated by slowing down traffic in advance both of which are not captured in macroscopic models. Safety benefits of VSL controllers such as reducing number of stops and reducing number of lane changes are demonstrated through VISSIM simulations. However, in order to get environmental benefits, VSL should be implemented in a way to force smoother speed profiles of individual vehicles. Simulation results also show that the effectiveness of VSL controllers are dependent on the traffic demand level and the congestion level. VSL controllers are more effective when traffic density is close to the critical density.

Chapter 1

Introduction

Variable speed limit (VSL) systems, as one of the freeway control strategies among Intelligent Transportation Systems (ITS) , have been studied since 1970s [43]. However, the cases of field implementations are limited, mostly in Europe and the U.S. through the use of roadside or overhead variable message signs (Figure 1.1 [35] and Figure 1.2 [1]). In the future VSL could be communicated directly to vehicles via short range infrastructure to vehicle communications and displayed in each vehicle for the driver to respond to or even in cases where the vehicles are operating under a cruise control or adaptive cruise control the vehicle could respond directly without the driver in the loop.

1.1 Problem

The VSL systems are considered to reduce risk of crashes, to warn drivers of hazardous roadway conditions, to stabilize and smooth traffic flows, to dampen shock waves, to postpone or prevent congestions, and to reduce emissions and fuel consumptions. The safety benefits of using VSL have been reported in several field studies both in Europe and the U.S. where the reduction in crashes were estimated to up to 30% [35]. Therefore, the incentive of using VSL has been mainly safety from the application point of view. However, benefits such as improved traffic flow

Figure 1.1: An example of roadside variable speed message signs

Figure 1.2: An example of overhead variable speed message signs

rates, lower travel times, smooth speed and density distribution and possibly lower pollution have been conjectured in literature and in some cases analyzed using mainly macroscopic traffic models. As most of the authors often admit, getting benefits in terms of travel times and higher traffic flows in a consistent manner using some of the adhoc VSL control techniques proposed is a challenge and stress the need for better VSL control strategies. The use of aggregate flow or macroscopic models and optimization techniques to develop and test dynamic VSL controllers which can be activated during incidents in addition to other situations let to some very optimistic results in terms of lowering travel times sometimes by as much as 20% [13]. A closer look at these results shows that using the same macroscopic model to design and test raises questions as to whether the simplicity of the models used for evaluation are responsible for these optimistic results given the fact that other studies using microscopic simulations fail to demonstrate improvements on travel times albeit for different VSL strategies. The question whether the VSL strategies or the macroscopic models used to analyze them or both are responsible for the large differences (not only quantitative but also qualitative) in traffic flow and travel time benefits reported, remains unanswered. Consequently, the problem of what are the most appropriate dynamic VSL controllers and what benefits can guarantee in a consistent manner under different traffic flow conditions is an open one.

In this study, the problems of the design, analysis and evaluation of dynamic VSL controllers will be addressed. A control engineering approach will be followed, where the control strategies are designed based on simplified models (in this case validated macroscopic traffic flow models) but applied and tested on validated microscopic traffic models under different traffic conditions. The dynamic VSL control design will be a proactive approach based on optimizing travel times, smoothness of traffic, environmental impacts and indirectly safety. As far as the author knows,

such a design that integrates all these possible benefits and constraints has not been addressed.

1.2 Existing Work

The simplest form of VSL is a fixed speed limit along the highway lanes which under normal road and weather conditions is the standard speed limit which could be lowered under bad weather conditions. What most people referred to as VSL is the display of different speed limits along the highway in response to traffic flow conditions.

There are two categories of VSL controllers, reactive or proactive. Reactive ones are those where current measured traffic states, speed, occupancy or flow, are compared with threshold values and the speed commands are selected from a predefined set [38, 3, 29]. To date, all the VSL systems that have been implemented or tested in the fields are reactive or switching logic based. On the other hand, for proactive controllers, the speed commands are optimized for the predicted traffic conditions based on some traffic flow models taking the current measurements and forecasted demands and events as inputs [9, 2, 12, 13, 32, 6, 21]. Therefore, there are two major design methods, the heuristic approach for the reactive controllers and the model-based optimization approach for the proactive controllers.

One of the earliest approaches is a heuristic switching logic based speed controller proposed in [38]. The possible values of VSLs are predefined, i.e., $\{90\ km/h, 80\ km/h, 70\ km/h\}$ and exercised according to certain thresholds of flow, speed and density. This approach was tested on a stretch of A2 motorway in the Netherlands [15]. Field experiment results demonstrate the homogenization effect of VSLs by showing reduced variations of flow, speed and occupancy across and within lanes. However, the results show no positive effect of VSLs on capacity or travel time. Furthermore, no results on the impact on safety and environment were

reported. The interesting question is whether the VSLs used were the most appropriate for the traffic conditions encountered. [3] presented a quantitative study of design and evaluation of an adhoc VSL control strategy using a crash model to assess safety. Microscopic (PARAMICS) simulation runs were conducted for different sets of thresholds and the results in terms of safety and travel time measurements were collected. The crash potential was quantified and used as a measure of safety. The simulation results showed reduced crash potential in most of the cases and negative impact on travel time in almost all of the cases considered. The authors observed that the VSL controller used was not robust over a wide range of traffic conditions in the sense of failing to provide consistent results in terms of safety and travel time and stressed the need of exploring alternative VSL controllers. In [7], a VSL controller is designed by treating the lanes at the beginning of each section as virtual ramps. The controller is a local proportional integral (PI) controller similar to ALINEA but is designed to operate as a speed limit controller. It is demonstrated using microscopic simulation runs that with this approach shock waves can be absorbed and travel times can be reduced when integrated with ramp metering. The results however were not consistent under different traffic conditions and improvements in travel time were small. In [29] real traffic data from a European motorway equipped with VSL were used to study the impacts of VSL on flow, density and speed using the fundamental diagram. The VSL controller had four settings that are no VSL, 60mph, 50mph and 40mph which are activated based on flow and speed thresholds and a ruled based algorithm. The real data involved clear days, rainy days and others. The results of the analysis show that there is no consistent indication that the flow capacity can increase as a result of VSL. This study did not include cases with incidents and large transients due to shock waves where VSL could have a more significant impact. Furthermore, the use of only three speed limits indicates a simplistic adhoc VSL controller. As the authors indicated the investigation of the VSL impact on aggregate traffic using real data

is difficult because data collected during specific VSL applications may not cover the whole range of possible traffic flow conditions. The authors also stressed the need for additional studies especially in the design of VSL and their location along the highway lanes.

In [32], a dynamic VSL control algorithm was proposed in an effort to absorb shock waves due to incidents and bottlenecks. The algorithm is developed using a distributed control approach based on minimizing the total time spent (TTS) in the network using a modified version of the macroscopic traffic flow model METANET. The dynamic VSL controller was designed and tested using the same model and showed improvements of about 20% with respect to TTS. A VSL controller is designed together with a ramp metering controller as part of a main stream traffic flow control strategy in [6] by minimizing a certain cost function that penalizes the TTS, ramp queue lengths, and large deviations in optimal control trajectories. The controllers are developed and tested using a modified version of the macroscopic traffic model METANET for an Amsterdam network. The results showed benefits in terms of TTS due to the use of VSL and ramp metering. Several other approaches use the macroscopic traffic flow model first proposed by Payne in [31], later modified by Papageorgiou in [27], and named as METANET ([25]) to develop VSL control strategies ([2, 12, 13, 32]). Due to the nonlinear and non-stationary behavior of freeway traffic, nonlinear model based optimization is often the design choice. Other approaches using similar macroscopic models include [26, 17, 8, 22].

The use of the macroscopic traffic model METANET and its variations for both design and testing raises questions regarding the applicability of the developed VSL strategies but more important whether similar benefits can be obtained in a more realistic traffic scenario using microscopic simulation runs for the following reasons. First the number of tests of VSL strategies using microscopic simulation runs are limited [3, 7] and these studies did not show any consistent improvements in TTS

as reported in the macroscopic model studies albeit the VSL controllers used were different.

Second the dynamic speed equation of the METANET model is an aggregate speed of flow in a section developed using a generalized car following model in [31] which does not take into account external inputs such as variable speed limit commands. In [6] and [14] efforts were made to modify the METANET model to account for VSL control inputs before it was used. Our investigation of these modifications using microscopic simulation studies show that while the METANET model can be tuned to match the aggregate characteristics of traffic flow with no VSL control the model fails to match the traffic flow in the presence of VSL control inputs suggesting that these modifications are not effective. The reason is that the inclusion of the VSL control inputs should be done by going back to car following considerations used to develop the macroscopic speed equation.

It was stated in several papers [6, 7] that the use of VSL control strategies will smooth the average density and speed distribution along the lanes and between lanes which is expected to have beneficial effects on the environment. As far as the author knows these statements have never been substantiated and are simple conjectures which may not be true for some VSL approaches. A VSL approach that slows down traffic for a longer period time may generate more pollution than without it in cases where larger changes in speed take place over a shorter period of time. The only way to evaluate these effects is by using microscopic simulation studies where the behavior of each vehicle is used by an appropriate emission model to calculate fuel consumption and emissions. A recent study by [5] on eco-driving shows the impact of speed control of one vehicle on emissions and fuel in dynamic traffic environments. They suggest that the infrastructure takes into account the environment and issue advisory commands to drivers in an effort to achieve more environmentally friendly driving behavior. In [37] the authors proposed what they call Intelligent Speed Adaptation (ISA). The function of ISA is to monitor the

position of the vehicle relative to the map of the road network using GPS, and compare its speed with the known static speed limit stored in the system. If the speed limit is exceeded, then ISA provides a warning to the driver to reduce speed, or if the driver does not respond then it does it automatically by not allowing the vehicle to exceed the speed limit. The study showed high benefits with respect to safety and in reducing carbon dioxides (CO2) emission and fuel consumption. With respect to travel time the study was inconclusive, since it relied only on abiding with static speed limits. In another emission and speed limit control study [44], model predictive controller is used with a longitudinal only vehicle following model (microscopic model) as both the prediction and simulation model.

1.3 Contribution

It is clear from reviewing most of the past efforts that:

- Field data from European highways as well as limited microscopic simulation studies where adhoc VSL control designs are implemented mainly for safety reasons do not show any consistent improvements in traffic flows and travel time which suggests that possibly more appropriate VSL strategies which take into account, in addition to safety, travel times, traffic flows and environmental impact need to be developed.

- Optimization techniques based on macroscopic traffic models are used to develop VSL controllers by a number of researchers. These controllers are evaluated using the same models claiming significant improvements up to 20% in some cases with respect to total travel time spent in the network. Since more realistic microscopic simulations have not been used to confirm these benefits and given the inability of these macroscopic models to mimic traffic in the presence of VSL commands, as the author found out, the levels of reported benefits remain in doubt.

- The environmental impact of VSL control has only been considered few of the studies reviewed. The design of VSL control strategies could take into account environmental effects and contribute to eco-driving as also suggested by some studies.

Motivated by the aforementioned questions and considerations, this study includes the design, analysis and evaluation of VSL control by following a controls engineering approach where control strategies are designed and analyzed using simplified models (in this case validated macroscopic models) but are tested and evaluated using more realistic complex models (validated microscopic simulation models), shown in Figure 1.3. Specifically the contribution of this report is:

- Developed a new VSL model to better describe the effects of VSL and to be used in the VSL controller design. All the existing models for incorporating effects of VSL are based on modifications of the steady state fundamental diagram. In this report, a new model derived from driver behaviors in case of VSL control is presented. The proposed model is validated using simulated data of microscopic models (VISSIM) and is compared to an existing macroscopic model modified to account for VSL. It is shown that the proposed model has more accurate descriptions of the transient effects of VSL than the existing model which has only take into account the steady state effects of speed control inputs.

- Addressed the model mismatch and uncertainty problems by testing the controller designed from simplified models (in this case validated macroscopic models) using more realistic complex models (validated microscopic VISSIM simulation models).

- Designed and analyzed a predictive VSL controller to minimize not only total travel time, but also variations of speed and density for the purpose of

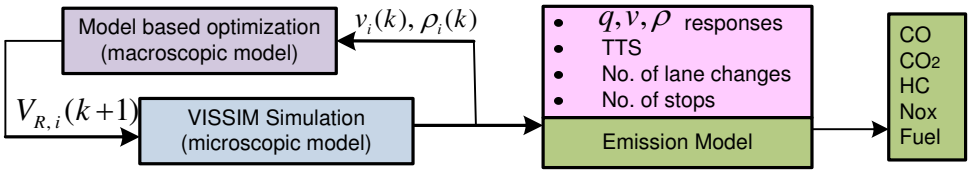

Figure 1.3: The VSL control design and evaluation system: flow of data

eco-driving subject to realistic constraints such as the temporal and spatial changes of VSL control inputs should within certain thresholds.

- Conducted comprehensive Monte Carlo simulation studies for different traffic scenarios to evaluate the robustness of the proposed controller and to examine the consistency of the potential environmental benefits, indirect safety benefits, and the benefits in improving smoothness and efficiency of traffic flow.

1.4 Outline

Chapter 2 presented the proposed new VSL model. The design and analysis of several VSL controllers are presented in Chapter 3. Chapter 4 is devoted to evaluations of the proposed controllers using an integrated simulation framework involving VISSIM. Conclusions are discussed in Chapter 5.

Chapter 2

Macroscopic Freeway Traffic Flow Models

2.1 Notations

A list of notations.

k	Simulation time step index, positive integer
T	Simulation time step length (in hours)
T_c	Controller time step length (in hours)
$\rho_i(k)$	Traffic density (in veh/km/lane) of section i at time kT
$v_i(k)$	Space mean speed (in km/h) of section i at time kT
$q_i(k)$	Traffic flow rate (in veh/h) leaving section i at time kT
$r_i(k)$	On-ramp inflow of section i at time kT
$s_i(k)$	Off-ramp outflow of section i at time kT
$V_{R,i}(k)$	Speed limit command of section i at time kT
L_i	The length (in km) of section i
λ_i	Number of lanes of section i

2.2 Macroscopic Traffic Flow Models

2.2.1 A New VSL Model

Continuum flow models describe traffic evolvement in terms of aggregated variables, i.e., flow, q, density, ρ, and speed, v. The LWR model ([20, 34]) is the first continuum flow model proposed in the literature using the similarity between freeway traffic stream and fluid. The LWR model is composed of three equations,

$$\rho_t + q_x = 0 \tag{2.1}$$

$$q = \rho v \tag{2.2}$$

$$q = Q(\rho) \tag{2.3}$$

where partial derivatives are denoted by subscripts; t is time and x is location; (2.1) is a first order nonlinear PDE from the conservation law; (2.2) is the relationship between the three aggregated traffic variables; and (2.3) is the steady state density-flow relationship, which is also called the fundamental diagram. For this first order model, speed $v(t, x)$ are approximated by the steady state speed $V_e(\rho)$, where $V_e(\rho) = Q(\rho)/\rho$. In effort to describe transient effects, Payne [31] extended the LWR model to a second order one by adding an acceleration equation (2.4) approximated from driver behaviors which is described by car following models in the case of no speed control.

$$v_t = \underbrace{-v_x v}_{\text{convection}} + \frac{1}{\tau}[\underbrace{V_e(\rho) - v}_{\text{relaxation}} - \underbrace{\frac{\mu \rho_x}{\rho}}_{\text{anticipation}}] \tag{2.4}$$

Consider a general car following model,

$$\ddot{x}_n(t+\tau) = \mathcal{F}(x_{n+1}(t), x_n(t), \dot{x}_{n+1}(t), \dot{x}_n(t)) \tag{2.5}$$

where $x_n(t)$ is the position of the n^{th} vehicle (the follower); $x_{n+1}(t)$ is the position of the $(n+1)^{th}$ vehicle(the leader), and τ is the reaction time. The above car following model describes the driver-vehicle behavior in case of no VSL control. When external speed commands are imposed (assume they are regulatory instead of advisory, otherwise, a noncompliance factor could be added), drivers, as the "actuators" of the system, will follow the commands and ignore the downstream traffic condition if it is safe to do so. Otherwise, drivers will follow the vehicle in front of them and ignore the speed commands. For example, if a vehicle is traveling at 70 km/h and the leading vehicle is not decelerating; at the same time, the displaying speed limit is 50 km/h, the driver will start to decelerate towards 50 km/h. If on the other hand, the leading vehicle is decelerating, the driver of the following vehicle will ignore the 50 km/h speed limit and start to decelerate with the leading vehicle towards a new safe headway. Once a new safe headway is reached, the driver will consider to follow the displaying speed limit if his/her speed is still above the speed limit. In other words, driver-vehicle behaviors switch between the car following mode and the speed limit tracking mode subject to safety constraints. Therefore, in addition to the car following model in (2.5), we propose to add a speed limit tracking model to describe the driver behaviors from which speed dynamic equation was derived. Speed limit tracking for n^{th} vehicle is approximated by a first order differential equation with delay τ,

$$\dot{V}_n(t+\tau) = a[V_R(t) - V_n(t)] = \mathcal{U}(V_R(t), V_n(t)) \tag{2.6}$$

where $V_R(t)$ is the speed limit and $a > 0$ is a model parameter. Drivers switch to the speed limit tracking mode from the car following mode when the VSL command is lower than the default speed limit, their own speed is above the VSL command, and the deceleration required by tracking the VSL command is less than that required

by following the vehicle in front. Therefore, we propose the driver behavior model as follows,

$$\dot{V}_n(t+\tau) = \begin{cases} \mathcal{U}(\cdot), & \text{if } V_R(t) < v_f \\ & \text{and } V_n(t) > V_R(t) \\ & \text{and } \mathcal{U}(\cdot) < \mathcal{F}(\cdot); \\ \mathcal{F}(\cdot), & \text{otherwise.} \end{cases} \tag{2.7}$$

where v_f is the free flow speed and also assumed to be the default speed limit. In [31], microscopic (2.5) was generalized to macroscopic speed dynamic equation (2.4). Similarly, (2.6) can be generalized to

$$v_t = a(V_R - v) = u(t,x) \tag{2.8}$$

Combine (2.4) and (2.8), the speed dynamic in case of VSL control is

$$v_t = \begin{cases} u(t,x), & \text{if } V_R < v_f \\ & \text{and } v > V_R \\ & \text{and } u(\cdot) < f(\cdot); \\ f(t,x), & \text{otherwise.} \end{cases} \tag{2.9}$$

where $f(t,x) = -v_x v + \frac{1}{\tau}[V_e(\rho) - v - \mu\frac{\rho_x}{\rho}]$ is the dynamics in case of no VSL control. For a freeway segment divided into N sections (Figure 2.1), discretize both

in time and space the second order macroscopic model with VSL control (2.9) and (2.1)-(2.3), our proposed new model is,

$$v_i(k+1) = v_i(k) + \begin{cases} u_i(k), & \text{if } V_{R,i}(k) < v_f \\ & \text{and } v_i(k) > V_{R,i}(k) \\ & \text{and } u_i(k) < f_i(k, d(k)); \\ f_i(k, d(k)), & \text{otherwise.} \end{cases} \tag{2.10}$$

where $v_i(k)$ is the speed of section i at time kT and T is the simulation time step length; $V_{R,i}(k)$ is the imposed variable speed limit in section i at time kT; and

$$u_i(k) = K_P[V_{R,i}(k) - v_i(k)] = K_P \cdot e_i(k) \tag{2.11}$$

$$e_i(k) = V_{R,i}(k) - v_i(k) \tag{2.12}$$

where $K_P > 0$ is a model parameter; and the term $f_i(k, d(k))$ derived from the car following model is

$$\begin{aligned} f_i(k, d(k)) = & \frac{T}{L_i} \frac{\rho_{i-1}(k)}{\rho_i(k+1) + \chi} v_{i-1}(k)[\sqrt{v_i(k) v_{i-1}(k)} - v_i(k)] \\ & + \frac{T}{\tau}[V_e(\rho_i(k)) - v_i(k)] \\ & - \frac{\mu(k) T}{\tau L_i} \frac{\rho_{i+1}(k - d(k)) - \rho_i(k)}{\rho_i(k) + \kappa} \\ & - \frac{\delta T}{L_i \lambda_i} \frac{r_i(k) v_i(k)}{\rho_i(k) + \kappa} \end{aligned} \tag{2.13}$$

where $\rho_i(k)$ and $r_i(k)$ are the density and on ramp flow of section i at time kT, respectively; L_i is the length of section i; λ_i is the number of lanes of section i;

$\chi, \tau, \delta, \kappa$ are model parameters; and $\mu(k)$ is a time varying model parameter and $d(k)$ is a time varying delay,

$$\mu(k) = \begin{cases} \mu_{high}, & \text{if } \rho_{i+1}(k) \geq \rho_i(k); \\ \mu_{low}, & \text{otherwise.} \end{cases} \tag{2.14}$$

$$d(k) = \begin{cases} d_{high}, & \text{if } \rho_{i+1}(k) \geq \rho_i(k); \\ d_{low}, & \text{otherwise.} \end{cases} \tag{2.15}$$

This switching VSL model is illustrated in Figure 2.2. The switching from car following mode to speed limit tracking mode only take place if the VSL command is lower than the default speed limit, lower than the current speed and if the change in speed is less than that of the predicted car following effects. In other words when the posted VSL is lower than the current speed the vehicles will respond without been influenced by the density and speed values of the vehicles ahead as vehicle following will switch to speed tracking without violating any safety considerations. Furthermore, comparing (2.13) to (2.4), several other modifications have been made:

- The original anticipation term suggests that a density change in the downstream section $i+1$ will impact section i in the next time step, which implies that shock wave has a *speed = section length/time step*. Section length is usually chosen as around 500 meters and time step is often chosen no greater than 10 seconds. Hence the shock wave speed is at least 180 km/h, which is quite unrealistic because shock wave speeds are about $15 - 25$ km/h [40]. Therefore, a delay time $d(k)T$, which is about the travel time of shock wave for the length of one section is added to the model when $\rho_{i+1}(k) \geq \rho_i(k)$, as shown in (2.15).

- Vehicle speeds are more affected by their downstream traffic and not so much by their upstream traffic. Therefore, we reduced the convection term in the dynamic speed equation as in [18].

- Speeds are impacted differently by the downstream queue formation and queue dissipation. Therefore, we change the anticipation coefficient μ from a constant to a time varying one as in [18] and [13].

- A ramp term modeling the on ramp merging effect is added as in [27].

The rest of this discrete second order model are,

$$\rho_i(k+1) = \rho_i(k) + \frac{T}{L_i\lambda_i}[q_{i-1}(k) - q_i(k) + r_i(k) - s_i(k)] \tag{2.16}$$

$$q_i(k) = \alpha\rho_i(k)v_i(k)\lambda_i + (1-\alpha)\rho_{i+1}(k-d(k))v_{i+1}(k-d(k))\lambda_{i+1} \tag{2.17}$$

$$V_e(\rho_i(k)) = \begin{cases} v_f, & \text{if } \rho_i(k) < \rho_c; \\ -\frac{v_f\rho_c}{\rho_j-\rho_c} + \frac{v_f\rho_c\rho_j}{\rho_j-\rho_c}\frac{1}{\rho_i(k)}, & \text{if } \rho_i(k) \geq \rho_c. \end{cases} \tag{2.18}$$

where $q_i(k)$ and $s_i(k)$ are flow and off ramp flow of section i at time step k, respectively; α is a model parameter; ρ_c and ρ_j are the critical density and jam density, respectively. A triangular fundamental diagram is adopted as estimated from VISSIM simulation data (Figure 2.3). The fidelity of our proposed model (2.10), (2.16),(2.17), and (2.18) is verified in the next section using microscopic simulations.

2.2.2 Boundary Conditions of the Model

The boundary conditions of the proposed model are specified by adding a source and a sink, i.e., section 0 and section $N+1$, respectively. For the source and the sink sections, a Cell Transmission Model concept is adopted from [11]. Section 0 is regarded as a "vehicle buffer", taking in demand q_d and discharging to section 1 at a rate q_0 not exceeding the flow section 1 can take nor the supply section 0 could

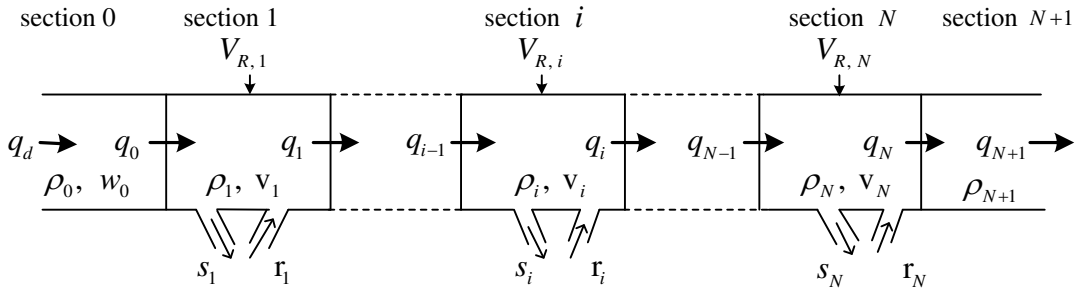

Figure 2.1: A freeway segment divided into N sections

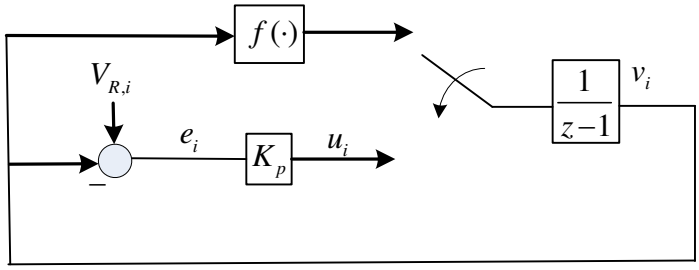

Figure 2.2: A switch model of VSL

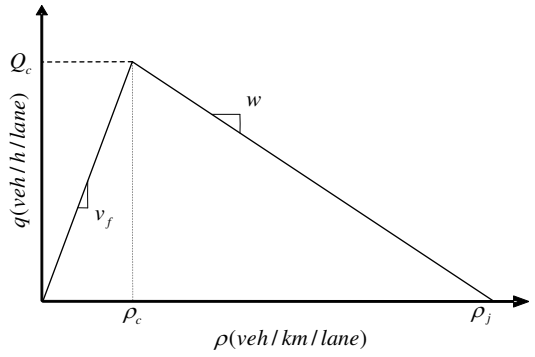

Figure 2.3: A triangular fundamental diagram

provide while holding any flow that is unable to enter section 1 as a mainline queue w_0.

$$q_0(k) = min\{q_d(k) + \frac{w_0(k)}{T}, Q_c, Q(\rho_1(k))\} \quad (2.19)$$

$$w_0(k+1) = w_0(k) + T(q_d(k) - q_0(k)) \quad (2.20)$$

where q_d is the flow demand; w_0 is the mainline queue length (in vehicles); Q_c is the capacity; and $Q(\rho_1(k))$ is the maximum flow that section 1 can take approximated from the fundamental diagram when the density of section 1 is $\rho_1(k)$. The speed of section 0 is assumed to be the same as that of section 1 so the convection term in (2.13) is zero for section 1. Section $N+1$ is assumed to have the same length and number of lanes as section N, and traffic in this section and its downstream sections are assumed to be free flowing. Therefore, flow and density of section $N+1$ follow:

$$q_{N+1}(k) = min\{\rho_{N+1}(k) v_f \lambda_{N+1}, Q_c\} \quad (2.21)$$

$$\rho_{N+1}(k+1) = \rho_{N+1}(k) + \frac{T}{L_N \lambda_N}(q_N(k) - q_{N+1}(k)) \quad (2.22)$$

2.2.3 Accident Scenario for Macroscopic Models

For a homogeneous multi-lane freeway segment shown in Figure 2.1, there are two ways to activate a bottleneck, an accident which causes temporary lane closure and a high demand from an on-ramp. For the sake of study VSL control, the ramps are assumed to have zero inflow. Various accident scenarios are created. It is not in their advantages to describe an accident for macroscopic models because it is difficult to model the effects of frequent lane changes both mandatary and discretional on the flow level while studies show that the lane change maneuvers may be the main cause of traffic instability and capacity drop [19, 24]. Although [19] attempted to model discretional lane changing for a first order traffic flow model,

there are no completed lane changing models for the second order flow model as far as the author knows. In this study, a microscopic model which incorporates a lane change model is used as the simulation model. To create accident scenarios for macroscopic model, the number of lanes of a section is simply reduced during a period of time. Since the downstream of the accident location is not in the interest of control, section N is chosen to be the section where the accident happens and some of lanes are closed. Equation (2.16) and (2.17) of section N are modified to be:

$$\rho_N(k+1) = \rho_N(k) + \frac{T}{L_N \lambda_N(k)}[q_{N-1}(k) - q_N(k)] \quad (2.23)$$

$$q_N(k) = \rho_N(k) v_N(k) \lambda_N(k) \quad (2.24)$$

where $\lambda_N(k)$ is the time varying available number of lanes of section N.

2.2.4 METANET and its Variations

Since METANET, the modified spatial and temporal discrete version of Payne's second order model [31], is quite popular for the design and simulation of traffic control strategies in the literature, it is presented here as follows,

$$\begin{aligned} v_i(k+1) &= v_i(k) \\ &\quad + \frac{T}{L_i}[v_i(k)v_{i-1}(k) - v_i(k)^2] \\ &\quad + \frac{T}{\tau}[V_e(\rho_i(k)) - v_i(k)] \\ &\quad - \frac{\mu T}{\tau L_i}\frac{\rho_{i+1}(k) - \rho_i(k)}{\rho_i(k) + \kappa} \\ &\quad - \frac{\delta T}{L_i \lambda_i}\frac{r_i(k)v_i(k)}{\rho_i(k) + \kappa} \end{aligned} \tag{2.25}$$

$$\rho_i(k+1) = \rho_i(k) + \frac{T}{L_i\lambda_i}[q_{i-1}(k) - q_i(k) + r_i(k) - s_i(k)] \tag{2.26}$$

$$q_i(k) = \rho_i(k)v_i(k)\lambda_i \tag{2.27}$$

$$V_e(\rho_i(k)) = v_f \exp[-\frac{1}{\alpha_m}(\frac{\rho_i(k)}{\rho_c})^{\alpha_m}] \tag{2.28}$$

where $\alpha_m > 0$ is a parameter of the parabolic fundamental diagram.

The existing research work modified the $V_e(\rho)$ term in the speed dynamic equation (2.4) to incorporate effects of VSL. One way to modify the equilibrium speed curve $V_e(\rho)$ is to scale the parameters of the curve, such as the free flow speed and the critical density, by the ratio of imposed VSL to the original speed limit ([9, 10, 38, 2, 12, 6]). Take the modification in [6] as an example, let $b_i(k) = \frac{V_{R,i}(k)}{v_f}$, the three parameters of $V_e(\rho_i(k))$ were rendered as follows,

$$\begin{aligned} v_f[b_i(k)] &= {v_f}^* b_i(k) \\ \rho_c[b_i(k)] &= {\rho_c}^*\{1 + A_m[1 - b_i(k)]\} \\ \alpha_m[b_i(k)] &= {\alpha_m}^*[E_m - (E_m - 1)b_i(k)] \end{aligned} \tag{2.29}$$

where ${v_f}^*$,${\rho_c}^*$,${\alpha_m}^*$ denote the specific non-VSL values of the parameters; A_m and E_m are constant parameters to be estimated from data. An illustration of the rendered fundamental diagram using (2.29)is shown in Figure 2.4.

Another modification of the curve is to replace $V_e(\rho)$ by the minimum of imposed VSL and the original $V_e(\rho)$, which was proposed in [14] as follows:

$$V_e(\rho_i(k)) = \min\left\{v_f \exp[-\frac{1}{\alpha_m}(\frac{\rho_i(k)}{\rho_c})^{\alpha_m}], (1+b)V_{R,i}(k)\right\} \tag{2.30}$$

where b is the non-compliance factor. An illustration of the rendered fundamental diagram using (2.30)is shown in Figure 2.5. A third modification ([22]) is to replace $V_e(\rho)$ by V_R.

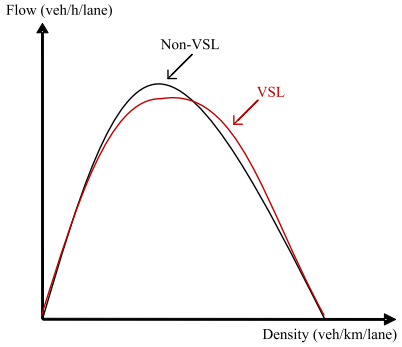

Figure 2.4: Rendered flow-density curves (1)

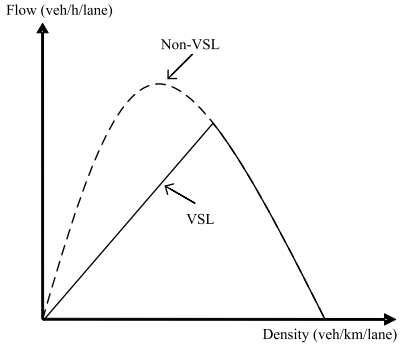

Figure 2.5: Rendered flow-density curves (2)

2.3 Model Validations

In this report, a unidirectional freeway stretch with $N = 10$ is considered. Two macroscopic models of the roadway, the proposed model and a METANET model used in [6] were constructed. The parameters of roadway geometry are set as follows,

- Total number of sections $N = 10$

- Section length $L_i = 500\ m,\ \forall i$
- Number of lanes $\lambda_i = 5,\ \forall i$

The parameters of simulation runs are set as follows,

- Total simulation time $= 60\ min$
- Simulation time step $T = 5\ s$
- VSL controller time step $T_c = 1\ min$

The parameters of the simulated traffic scenario are set as follows,

- Traffic mainline demand $q_d = 1800\ veh/h/lane$
- Traffic on-ramp demand $r_i = 0\ veh/h/lane,\ \forall i$
- Traffic off-ramp outflow $s_i = 0\ veh/h/lane,\ \forall i$
- Accident in section 10 with 2 lanes out of 5 lanes closed during 5-15 min, i.e.,

$$\lambda_{10}(k) \begin{cases} 3, & \text{if } 5\ min < kT < 15\ min; \\ 5, & \text{otherwise.} \end{cases} \tag{2.31}$$

A third model, the microscopic simulation model is constructed using VISSIM (details will be explained in Chapter 4), of which the model parameters were validated using field data from the Berkeley Highway Laboratory (BHL) [39]. The other parameters, such as that of the roadway, simulation runs, and traffic scenarios, are set to the same as those of the two macroscopic models. The two macroscopic models were calibrated against VISSIM simulated speed, density and flow data. For example, a triangular fundamental diagram (2.18) is used for both of the macroscopic models and its parameters, free flow speed $v_f = 105\ km/h$, critical

Parameter	*Unit*	Proposed Macro-model	METANET
τ	*second*	5	18
κ	*veh/km/lane*	50	40
μ	km^2/h		60
μ_{high}	km^2/h	25	
μ_{low}	km^2/h	15	
d_{high}	*second*	60	
d_{low}	*second*	20	
χ	*veh/km/lane*	4	
α		0.8	
v_f	*km/h*	105	105
ρ_c	*veh/km/lane*	22	22
ρ_j	*veh/km/lane*	145	145
K_P		0.5	
A_m			1.5

Table 2.1: Validated macroscopic model parameters

density $\rho_c = 22\ veh/km/lane$, and jam density $\rho_j = 145\ veh/km/lane$ were estimated from VISSIM data (shown as red points in Figure 2.6). All the calibrated model parameters are shown in Table 2.1.

For the VISSIM model, the VSL commands are communicated to vehicles at the beginning of each section and all the drivers are assumed to comply with the imposed VSL commands. During the one hour long simulation run, an accident is introduced in section 10 (the most downstream section) that led to two lanes been closed over the time interval 5 to 15 minutes which led to the activation of some hypothetical VSL inputs been issued to lower speeds in section 6-9. The VSL extensions of the two macroscopic models were also validated using VISSIM simulation data. In (2.12), $K_P = 0.5$. To validate the VSL extension of the METANET model, dozens of VISSIM simulation runs were conducted by imposing different speed limits through the whole simulation run. For example, speed limit is set to be 80 km/h for all the sections and for the whole one-hour simulation to get near stationary measurements of density and speed. As shown in Figure 2.6, (red, blue, yellow and green points are from non-VSL, $V_R = 80\ km/h$, $V_R = 60\ km/h$, and $V_R = 40\ km/h$ data, respectively), parameters v_f and ρ_c change with speed limits. By regression, the estimated $A_m = 1.5$ in (2.29).

2.3.1 Model Comparison

Some hypothetical VSL commands are issued during the accident time (5 to 15 minutes), as shown in Figure 2.7. To demonstrate the goodness of fit of the proposed model, simulated speeds of the three validated models, VISSIM, the proposed macroscopic model and the METANET were compared. Figure 2.8 shows typical speed responses from section 9 which was one section upstream of the accident on top of the VSL commands. It is clear that the two macroscopic models match very well the microscopic flow in the absence of VSL commands. When the VSL commands are activated the model of [6] deviates considerably from the VISSIM

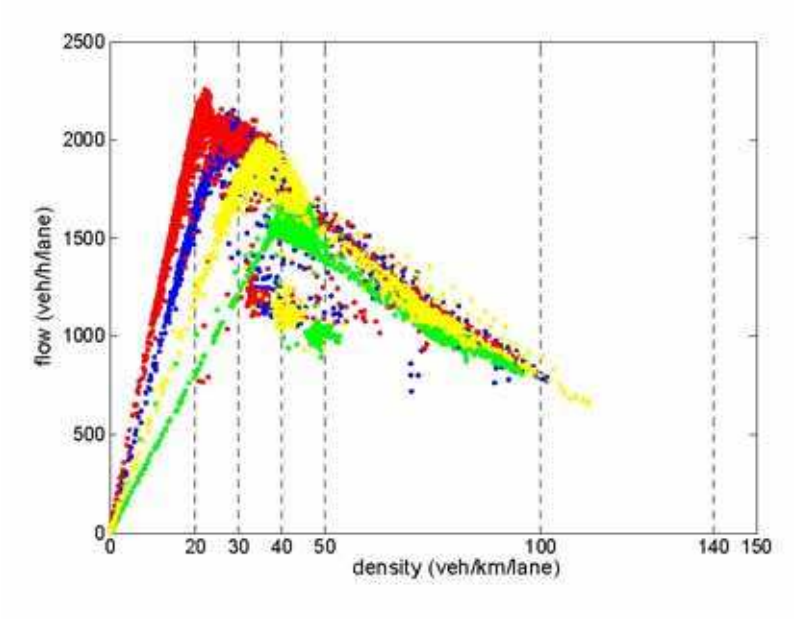

Figure 2.6: The density-flow curves from VISSIM data: (a)No-VSL (red),(b)VSL = 80 km/h (blue), (c)VSL = 60 km/h (yellow),(d)VSL = 40km/h (green)

response whereas the proposed model in this paper follows pretty well the VISSIM response. The same consistent comparisons are observed for the other sections for both speed and density as well as for other hypothetical VSL commands and incident scenarios considered. This comparison indicates that the proposed macroscopic model is more appropriate for taking into account VSL commands than the usual METANET model and some of its recent modifications. It is therefore more appropriate for designing VSL controllers and analyzing their properties before testing them using more realistic microscopic simulation models.

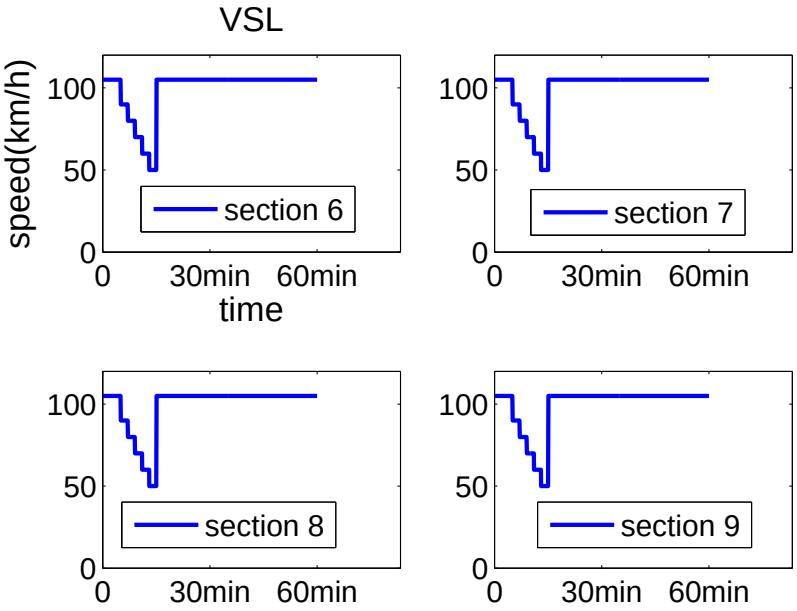

Figure 2.7: Some hypothetical VSL commands

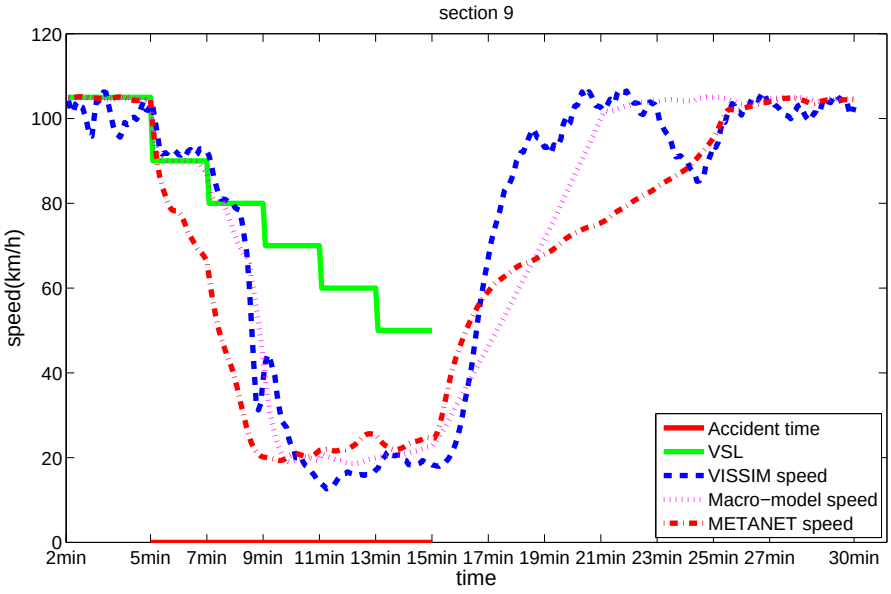

Figure 2.8: Simulated speed responses of the three models considered

Chapter 3

Controller Design

3.1 Mainline Virtual Metering-A simple VSL control

3.1.1 Controller Design

ALINEA is a simple local ramp metering strategy based on pure integral control action. Different studies have demonstrated that ALINEA is non-inferior to sophisticated coordinated approaches under recurrent traffic congestion ([28]). ALINEA can be expressed as

$$R(k) = R(k-1) + K_r[O_d - O(k)] \tag{3.1}$$

where $R(k)$ is the ramp meter command at time step k, K_r is a control parameter (integral gain), $O(k)$ is the measured immediate downstream occupancy at time step k, and O_d is the desired value for the downstream occupancy which is typically chosen close to the critical occupancy O_c ([28]). Since inductive loop detectors are still the most common sensors used in the field and only occupancy is measurable by inductive loop detectors, ALINEA is implemented using the occupancy instead of density. The control strategy described by (3.1) is a simple integral regulator where the integral action rejects constant disturbances and tracks constant reference points in an effort to force the downstream occupancy to stay close to the

desired occupancy when traffic volume is high. We generalize the ALINEA ramp metering strategy to a simple speed control based on the fundamental flow-density relationship. Section i is regarded as a virtual on ramp of section $i+1$ and the same integral control strategy as in the case of ramp metering is applied to regulate the metered flow rate Q_i from section i to section $i+1$, i.e.,

$$Q_i(k) = \begin{cases} Q_{max}, & \text{if } \bar{Q}_i(k) > Q_{max}, \\ Q_{min}, & \text{if } \bar{Q}_i(k) < Q_{min}, \\ \bar{Q}_i(k), & \text{otherwise.} \end{cases} \tag{3.2}$$

where

$$\bar{Q}_i(k) = Q_i(k-1) + K_v\Big\{\rho_d - \frac{1}{N_{r,i}} \sum_{j \in I_{r,i}} \rho_j(k)\Big\} \tag{3.3}$$

where ρ_d is the desired density for speed control; $I_{r,i}$ is the set of relevant sections to section i; $N_{r,i}$ is the number of sections in the set $I_{r,i}$; and $K_v > 0$ is a controller parameter. ALINEA is a local ramp metering where the immediate downstream occupancy is compared with the desired occupancy. For the mainline virtual ramp metering, the immediate downstream density of section i, i.e., $\rho_{i+1}(k)$, might not be enough. Therefore, the average density of several downstream sections of section i is compared with the desired density, i.e., the sections in set I_r. (3.2) and (3.3) provide the regulation of the flow at the beginning of a particular section of the highway. This flow rate control strategy cannot be implemented as done in the case of ramp metering, because in this case the control variable is the speed. Therefore, in order to regulate traffic speed instead of the traffic flow rate, we map a flow command into a speed command using the flow-speed relationship as described by the fundamental flow-density diagram, shown in Figure 3.1. It is only reasonable to set upper and lower bounds on the speed commands of section i, $V_{R,i}(k)$, i.e.,

$$V_{min} \leq V_{R,i}(k) \leq V_{max} \tag{3.4}$$

where V_{max} is the maximum speed limit allowed, which is often set to be the default speed limit, and V_{min} is the lowest dynamic speed limit we want to apply. Therefore, we set Q_{min} as the flow corresponding to V_{min}. Because the capacity flow is usually not achieved at the maximum speed allowed, we set Q_{max} as the flow corresponding to the critical density which is the capacity flow. Denote the speed corresponding to the critical density as $V_{critical}$, and we have $V_{min} < V_{critical} < V_{max}$. The curve between point A and point B in Figure 3.1 is a mapping from $[Q_{min},\ Q_{max}]$ to $[V_{critical},\ V_{min}]$. In this study, a triangular fundamental diagram is used. Therefore, the mapping from flow to speed becomes

$$\bar{V}_{R,i}(k) = \frac{v_f \rho_c Q_i(k)}{v_f \rho_c \rho_j - (\rho_j - \rho_c) Q_i(k)} \tag{3.5}$$

However, $\bar{V}_{R,i}$ generated by (3.5), (3.2) and (3.3), may lead to unsafe changes of speed limits. For practical purposes, we use the following speed limit V_i which is smoother.

$$V_{R,i}(k) = \begin{cases} V_{R,i}(k-1) - C_v, & \\ & \text{if } \bar{V}_{R,i}(k) \leq V_{R,i}(k) - C_v \\ V_{R,i}(k-1) + C_v, & \\ & \text{if } \bar{V}_{R,i}(k) \geq V_{R,i}(k) + C_v \\ \bar{V}_{R,i}(k), & \text{otherwise.} \end{cases} \tag{3.6}$$

where C_v is a positive constant represented the biggest changes of speed commands allowed. In this report, $C_v = 10\ km/h$.

3.1.2 Macroscopic Simulation Model Calibration

Taking advantages of the simplicity and computational benefit of macroscopic simulations, the proposed VSL controller is tuned and tested first using macroscopic

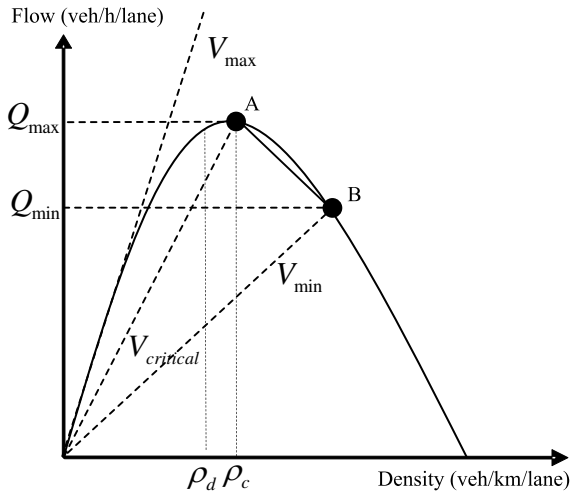

Figure 3.1: Mapping flow to speed

simulations. The proposed macroscopic simulation model in Chapter 2 is calibrated against simulated density and speed from VISSIM simulations. The roadway model is the benchmark model used in Chapter 2, which is a 5km freeway segment without ramps, divided into 10 500m-long sections each of which is homogenous with 5 lanes. Both of the VISSIM and the macroscopic simulations have the same mainline demands of 1800 $veh/h/lane$, which is close to the capacity of 2100 $veh/h/lane$. The accident scenarios created are the same for both models, i.e., two lanes closed during 5-15min in section 10, which is the most downstream section of the freeway segment. Figure 3.2 shows simulated density and speed of the VISSIM simulation and that of the calibrated macroscopic model. Compare Figure 3.2(a) and Figure 3.2(c), density of section 10 from macroscopic simulation is much higher than that of VISSIM simulation. This is because in VISSIM, the lane is only blocked at one point, and the space of the rest of the lane is still available to hold vehicles. While in macroscopic models, the whole 500m space is taken out to model one lane closure. Moreover, except section 10, the maximum density of every section is generally higher in VISSIM simulations. This is because in VISSIM, vehicles change back and forth between fast and slow lanes which cause more interruptions to traffic

flow, while congestion only comes from the fact that demand is over supply because of two lane closed in macroscopic simulations. Compare the simulated speeds in Figure 3.2(b) and Figure 3.2(d), speed of section 10 is constant from VISSIM to macroscopic model. Similarly to the density, speed is lower from VISSIM simulation than from macroscopic simulation. The accident creates shock waves that propagate upstream from section 10. To compare the shock wave behavior of the two models, the density and speed contour are plotted in Figure 3.3. It is shown that the shock wave dissipate around section 2 or 3 for both models. However, the shock wave has longer impact for every section for the macroscopic model.

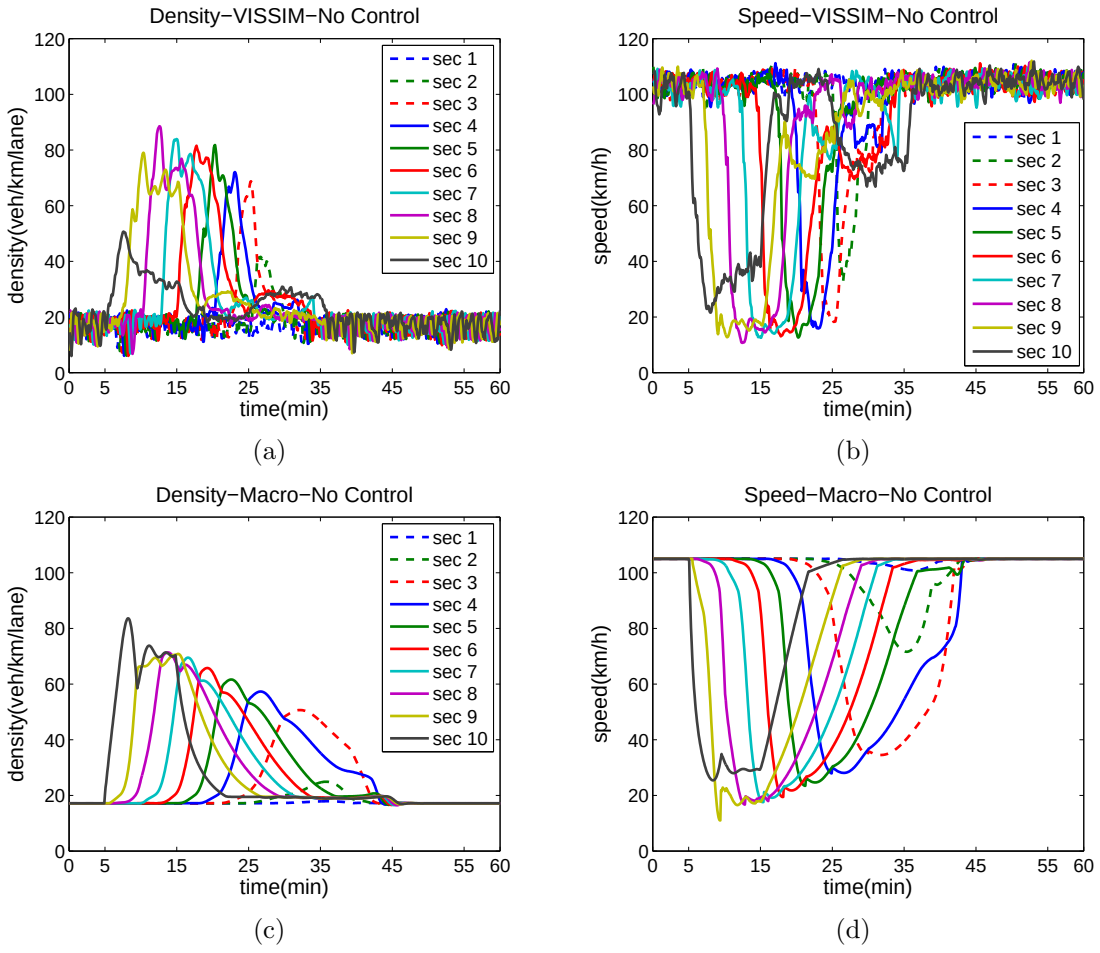

Figure 3.2: Calibration of macroscopic simulation model: (a) VISSIM simulated density, (b) VISSIM simulated speed, and (c) Macro simulated density, (d) Macro simulated speed.

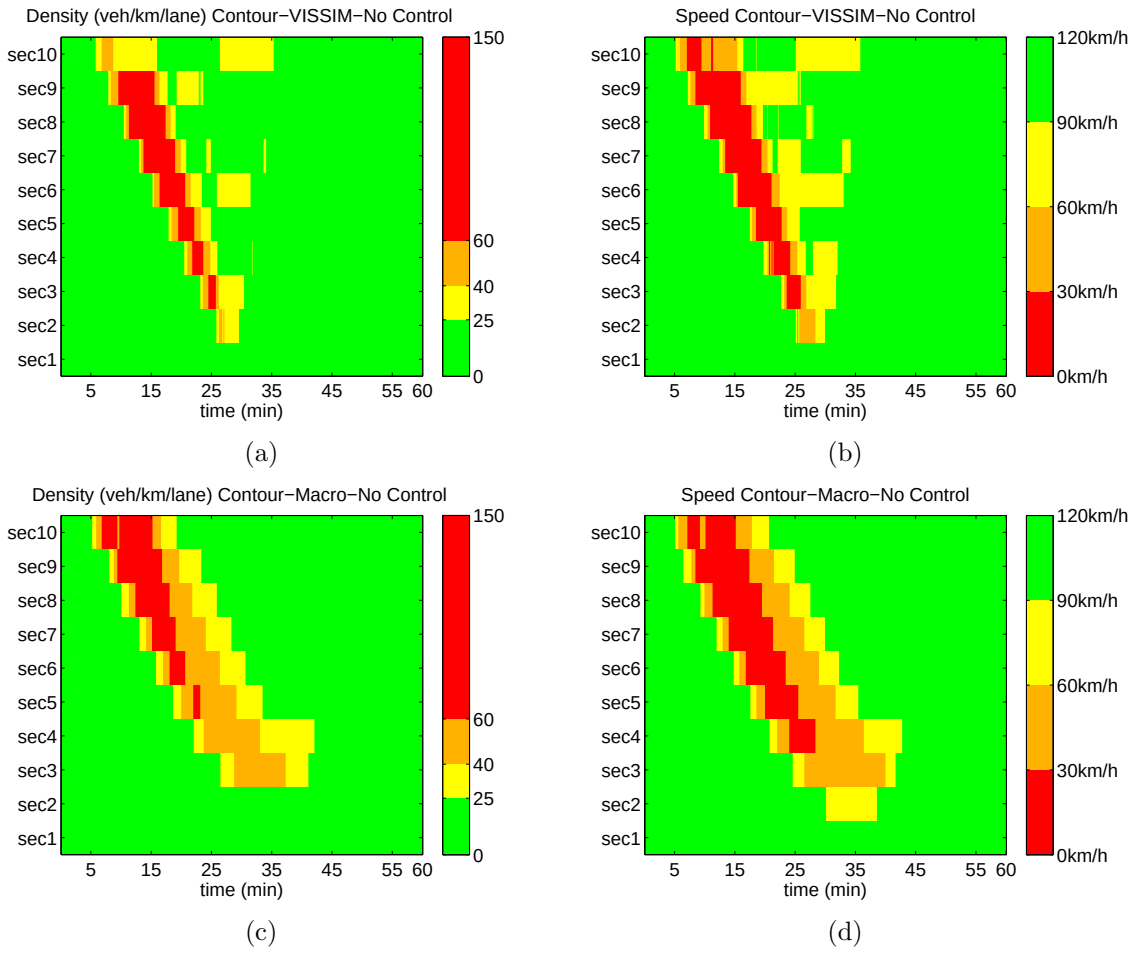

Figure 3.3: Calibration of macroscopic simulation model: (a) VISSIM simulated density, (b) VISSIM simulated speed, and (c) Macro simulated density, (d) Macro simulated speed.

3.1.3 Macroscopic Simulations

The proposed simple VSL controller is tuned and tested with the calibrated macroscopic simulation model. The accident is in section 10 from 5min to 15min. The controlled sections are section 4-9 and the VSL controller is active from 5min to 15min. Figure 3.5 shows the generated control signal. The no control and controlled density and speed are shown in Figure 3.4. Except section 10, maximum density for each section is reduced by the VSL control. For example, the peak density of

section 9 is around 70 $veh/km/lane$ when there is no control and is reduced to around 40 $veh/km/lane$ by VSL control. The duration of congestion is reduced too. Speed goes back to free flow speed around 45min when there is no control, while recover around 40min with control. Figure 3.6 shows that the shock wave is suppressed by the controller too. The TTS is estimated to be reduced by 5% with control (shown in Table 3.1).

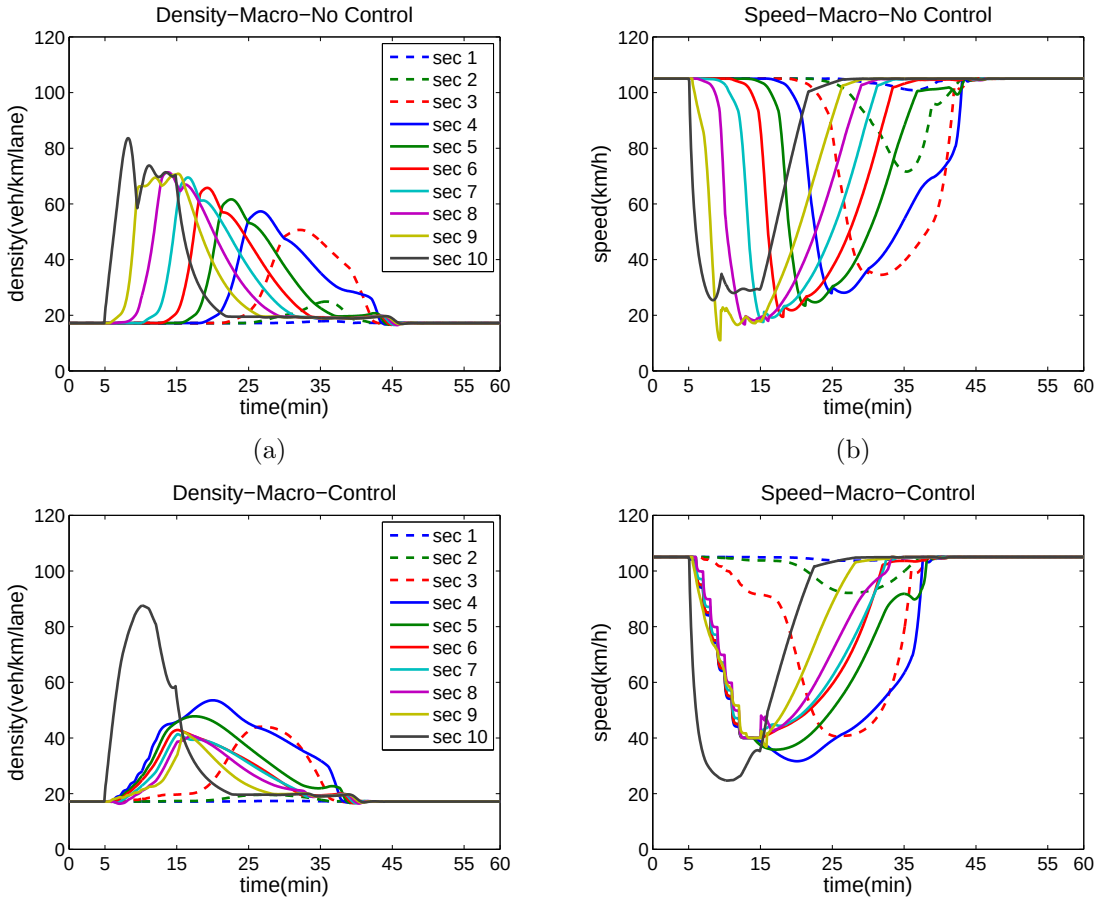

Figure 3.4: Macroscopic simulation: No control (a) density, (b) speed, and Simple VSL controller (c) density, (d) speed.

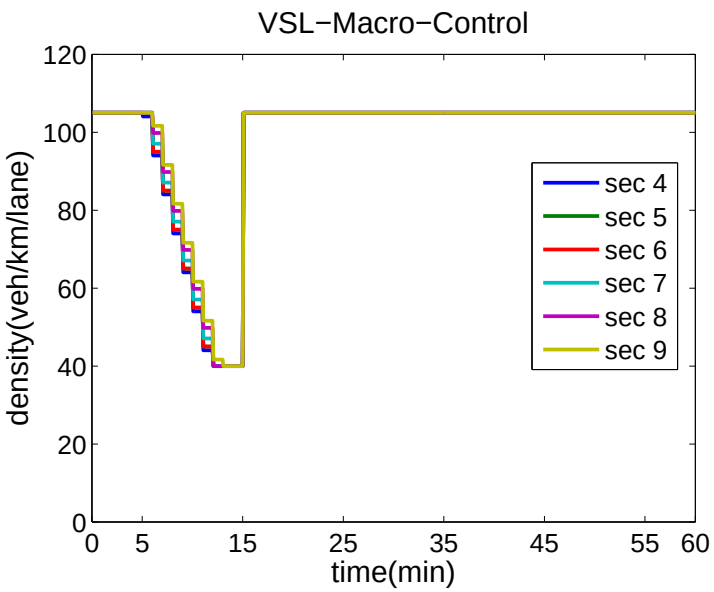

Figure 3.5: Macroscopic simulation for simple VSL controller: VSL commands

3.2 Nonlinear Model Predictive VSL Control

3.2.1 Controller Design

Reactive VSL control strategies, such as the one presented in 3.1 could be helpful to some extent. However, the desired density ρ_d need to be adjusted to different traffic scenarios. Moreover, once congestion is built up, the off-ramps may even be blocked, there is not much effective control action possible but to wait for the queues to dissipate. Hence, applying control actions on the onset of congestion or even in advance of anticipated congestion to prevent traffic flow from break down is necessary and effective. To make such proactive control decisions, predictions of the traffic states into the near future need to be made. In fact, the idea of proactive control is intuitive. Experienced commuters make their decisions on when to depart or which route to take based on their anticipations about the traffic conditions. Their "experience" is a model that they generalized from data they have collected in the past. In this report, the proposed traffic flow model incorporating VSL

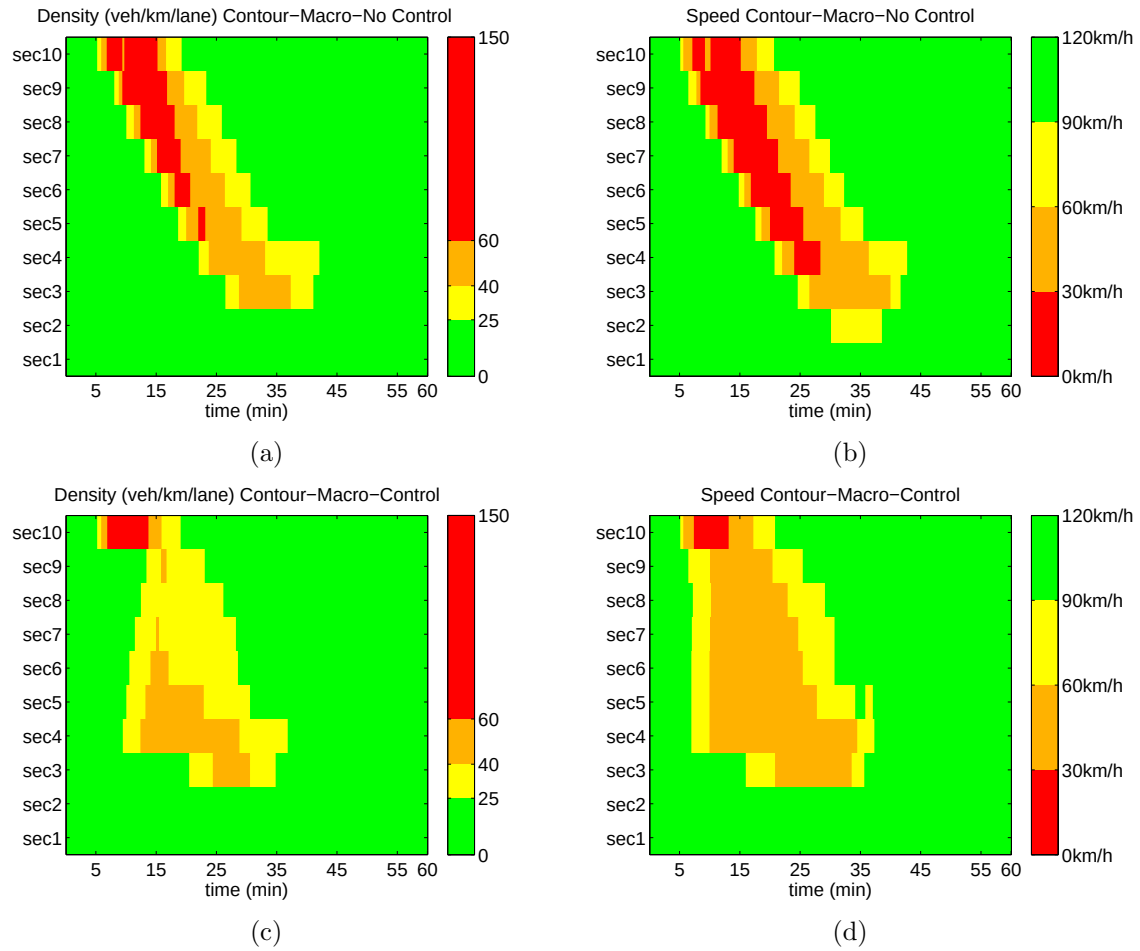

Figure 3.6: Macroscopic simulation: No control (a) density contour, (b) speed contour, and Simple VSL controller (c) density contour,(d) speed contour.

effects is used to predict traffic evolvement in the present of VSL control and hence a nonlinear model predictive controller is designed to attempt to optimize traffic flow through the use of variable speed limits.

For this VSL control problem, the nonlinear model predictive control (NMPC) is formulated as solving on-line a finite horizon open-loop optimal control problem subject to system dynamics and constraints involving states and controls, predicted demands and events. Dynamics of the freeway traffic system involving VSL controls are described by the proposed macroscopic traffic flow model. Future mainline demands and ramp flows are forecasted through historical traffic data and current

traffic states measurements. Events, such as the lane closure duration, could be generated from a probability distribution. Specifically, as illustrated in Figure 3.7, based on measurements of speed and density obtained up to time $k \cdot T$ and the forecasted demands/events predetermined at time $k \cdot T$, the controller predicts the future speed and density over a prediction horizon $P \cdot T$ and determines (over a control horizon $P_c \cdot T_c \leq P \cdot T$ the VSL commands such that a predetermined open-loop performance objective function J is optimized. Considering the model mismatch, the uncertainty in the future demands/events, and the possibility that the optimization problem could not be solved in time, the calculated open loop V_R are only implemented for one controller time step T_c. Hence, using the new measurements and forecasted demands/events at time $k \cdot T + T_c$, the whole procedure-prediction and optimization-is repeated to find new VSL commands. Here, T is the surveillance system sampling period or the time step size for the discrete time macroscopic model, normally, around 5 to 10 seconds; k is a time step index. T_c is the controller sampling period, i.e., the VSL commands could change every T_c seconds. For practical purpose, T_c should not be too small, we use $T_c = 60$ *seconds*.

3.2.2 Cost Functions

In addition to the safety benefit that has been shown in the field implementations, VSL control is aiming at alleviating congestion and reducing pollution and energy consumption. Total Time Spent (TTS), which is the total time all the vehicles spent in the network for a certain time period, is often used to quantify congestion.

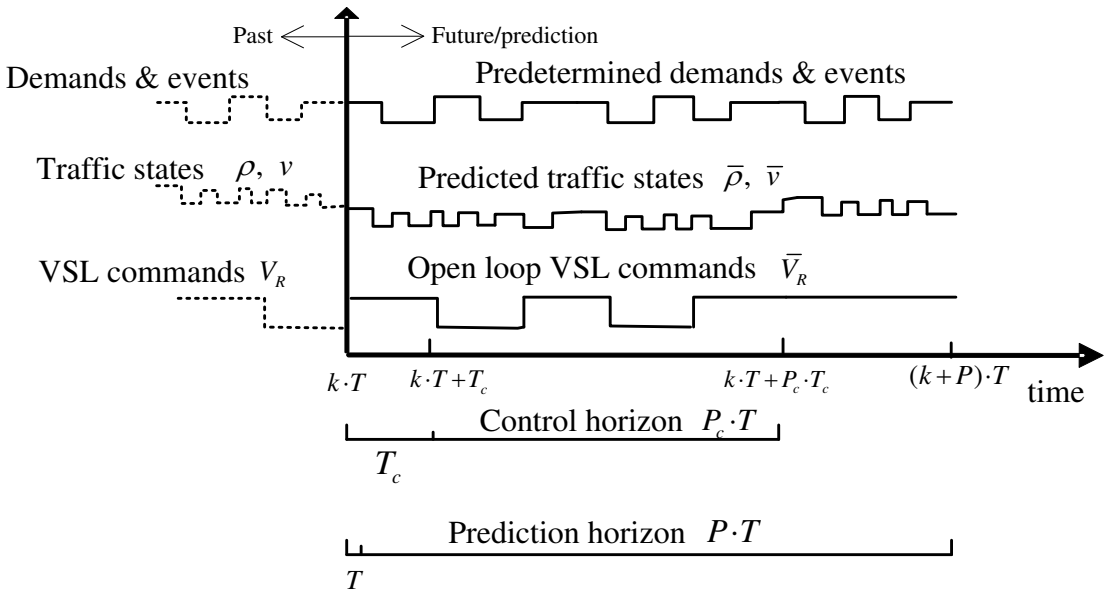

Figure 3.7: Principle of nonlinear model predictive VSL control

Moreover, VSL commands for a section should change smoothly for practical purpose. Therefore, for cost function J_1, TTS and sum of the squares of the changes in VSL commands for all the controlled sections over the control horizon are included.

$$\begin{aligned} J_1(k) &= w_1\Big\{T\sum_{j=k+1}^{k+P}\sum_{i=1}^{N}\rho_i(j)L_i\lambda_i + T\sum_{j=k+1}^{k+P}w_o(j)\Big\} \\ &\quad + w_2\Big\{\sum_{j=k}^{k+P_c-1}\sum_{i\in I_c}[V_{R,i}(j+1) - V_{R,i}(j)]^2\Big\} \end{aligned} \tag{3.7}$$

where P is the prediction horizon; N is the number of sections; P_c is the control horizon; w_1 is the weight for the total travel time; w_2 is the weight for the total changes of VSL; and I_c is the set of controlled sections. In [5], it is shown that if a vehicle avoids frequent acceleration and deceleration while travels as fast as possible, the fuel consumption and CO2 emissions could be reduced. System-widely, minimizing only the total travel time will not necessarily result in less fuel consumption or pollution because the smoothness of vehicle speed profiles are not

considered. Therefore, to achieve the system-wide eco-driving, it is necessary to minimize both travel time and some quantity which is an indicator of the vehicle acceleration. Only aggregated traffic states such as, link speed (space mean speed) and link density are available from macroscopic models. For example, shown in Figure 3.8 is the speed contour of the one hour simulation for the 10-section freeway segment illustrated in the figure. The space-time plane is divided into small identical cells with the the length in y direction as 500 meters, and 5 seconds in the x direction. The color of each cell represents its average speed, as low speed showing in red and free flowing speed showing in green. Based on this speed contour, we could create a hypothetical vehicle trajectory given the speed of each cell that the vehicle travels through. In the figure, such a trajectory shows that if a vehicle enters section 1 at around 15 minute, it would travel at free flow speed until it meets the end of the queue and starts to slow down. After it goes through the shock wave region and enters section 8, it starts to recover its speed and leaves the freeway segment before just before the 25 minute. If there are no congestion, it takes the vehicle less than 3 minutes to travel through the 5 km freeway segment, while it takes this "hypothetical" vehicle about 10 minutes. This example shows that the "hypothetical" vehicle speed profile based on the aggregated speed measurements could be used to approximate vehicle acceleration. If the "hypothetical" vehicle is in cell $(k,\ i)$, (illustrated in Figure 3.9), its speed $(v_i(k))$ could change when it enters the next cell $(k+1,\ i)$ or $(k+1,\ i+1)$. Therefore, $[v_i(k+1)-v_i(k)]^2$ and $[v_{i+1}(k+1)-v_i(k)]^2$ quantify the possible acceleration of the "hypothetical"

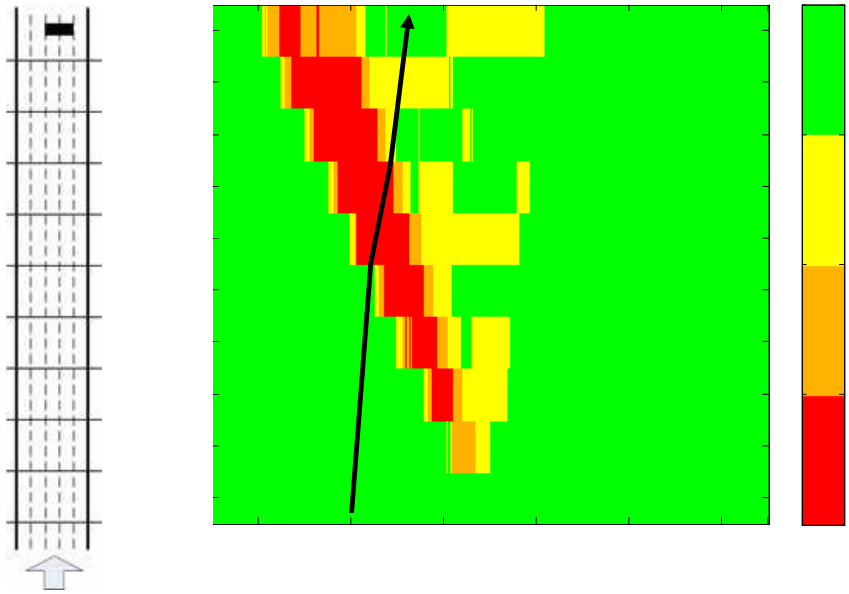

Figure 3.8: Speed contour and an estimated vehicle trajectory

vehicle. The sum of the aforementioned quantities for all the cells are therefore included into the cost function J_2.

$$\begin{aligned} J_2(k) \;=\; & w_1\Big\{T\sum_{j=k+1}^{k+P}\sum_{i=1}^{N}\rho_i(j)L_i\lambda_i + T\sum_{j=k+1}^{k+P} w_o(j)\Big\} \\ & + w_2\Big\{\sum_{j=k}^{k+P_c-1}\sum_{i\in I_c}[V_{R,i}(j+1)-V_{R,i}(j)]^2\Big\} \\ & w_3\Big\{\sum_{j=k}^{k+P-1}\sum_{i=1}^{N}[v_i(j+1)-v_i(j)]^2\Big\} + w_4\Big\{\sum_{j=k}^{k+P-1}\sum_{i=1}^{N-1}[v_{i+1}(j+1)-v_i(j)]^2\Big\} \end{aligned} \tag{3.8}$$

where w_3 and w_4 are the weights.

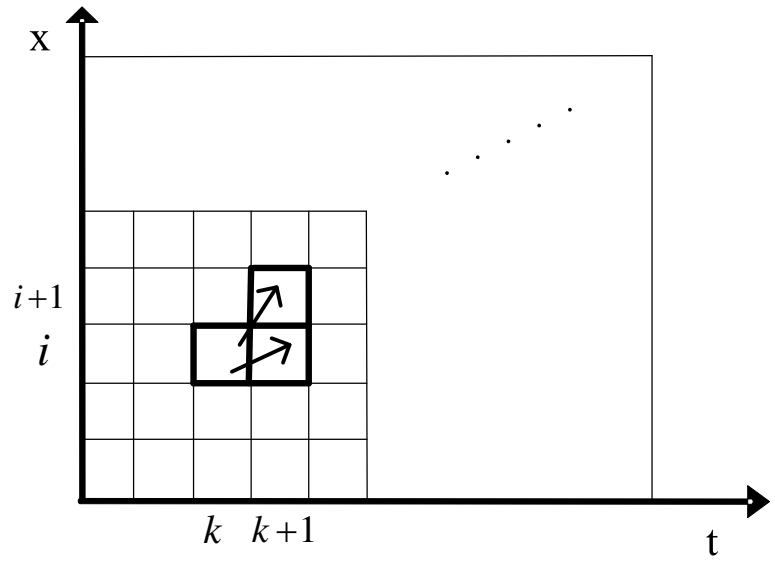

Figure 3.9: Approximation of vehicle acceleration on the macroscopic level

3.2.3 Constraints

The constraints on VSL commands are from the consideration of safe operations. For example, it is not safe to ask a vehicle to decelerate to 50 km/h if it is traveling at 90 km/h. The VSL commands along a vehicle trajectory should only be reduced within some threshold $C_v > 0$. As shown in Figure 3.9, the difference of VSL commands of cell $(k+1,\ i)$ or $(k+1,\ i+1)$ and cell $(k,\ i)$ should be constrained. Therefore, we have the following constraints for the optimization problem,

$$V_{R,i}(j) - V_{R,i}(j+1) \leq C_v, \quad \forall i \in I_c, \quad \forall j \in [k, ..., k+P_c-1] \tag{3.9}$$

$$V_{R,i}(j) - V_{R,i+1}(j+1) \leq C_v, \quad \forall i \in I_c, \quad \forall j \in [k, ..., k+P_c-1] \tag{3.10}$$

$$V_{min} \leq V_{R,i}(j) \leq V_{max}, \qquad \forall i \in I_c, \quad \forall j \in [k, ..., k+P_c] \tag{3.11}$$

3.2.4 Macroscopic Simulations

In this chapter, the two NMPC VSL controller are tested using macroscopic simulations, i.e., the same macroscopic model that the controller used to predict traffic states. Therefore, there are no model mismatch or uncertainty involved. The optimization problem is solved by MATLAB function "fmincon" which uses a sequential quadratic programming (SQP) method. The prediction horizon is $P \cdot T = 10\ min$; the control horizon is $P_c \cdot T_c = 4\ min$; section 4-9 are controlled and the controller is activated when the lanes are blocked, i.e., 5min to 15min. The lowest speed limit allowed $V_{min} = 30\ km/h$, and the VSL are rounded to the nearest integer when applied; the biggest gap of VSL allowed is $C_v = 10\ km/h$. The performance measurements used are TTS (and equivalently, average speed per vehicle) and smoothness, which is

$$S = \sum_{k=1}^{K_t-1} \sum_{i=1}^{N} [v_i(k+1) - v_i(k)]^2 + \sum_{k=1}^{K_t-1} \sum_{i=1}^{N-1} [v_{i+1}(k+1) - v_i(k)]^2 \tag{3.12}$$

where K_t is the number of total simulation steps, $K_t \cdot T = 1\ hour$p; $N = 10$ is the total number of sections. These performance measurements and their difference from those of the no controlled case are shown in Table 3.1. For all the three controllers tested, TTS is almost unchanged but smoothness are improved for up to 36%. The generated control signals are shown in Figure 3.10. As shown in the density and speed contour plots in Figure 3.11, shock waves are suppressed a little bit by the controllers.

3.3 Proportional Speed Controller

3.3.1 Controller Design

To further simply the mainline virtual metering speed controller in section 3.1,we propose a proportional speed limit controller which is also inspired by ALINEA and

Table 3.1: Macroscopic Simulation Results

	TTS (hours)	Difference	Average Speed per vehicle (km/h)	Difference	Smoothness	Difference
No control	595.339		75.6		292	
Simple controller	563.6322	-5%	79.8	6%	187	-36%
NMPC J_1	587.3899	-1%	76.6	1%	235	-20%
NMPC J_2	583.2437	-2%	77.2	2%	218	-25%

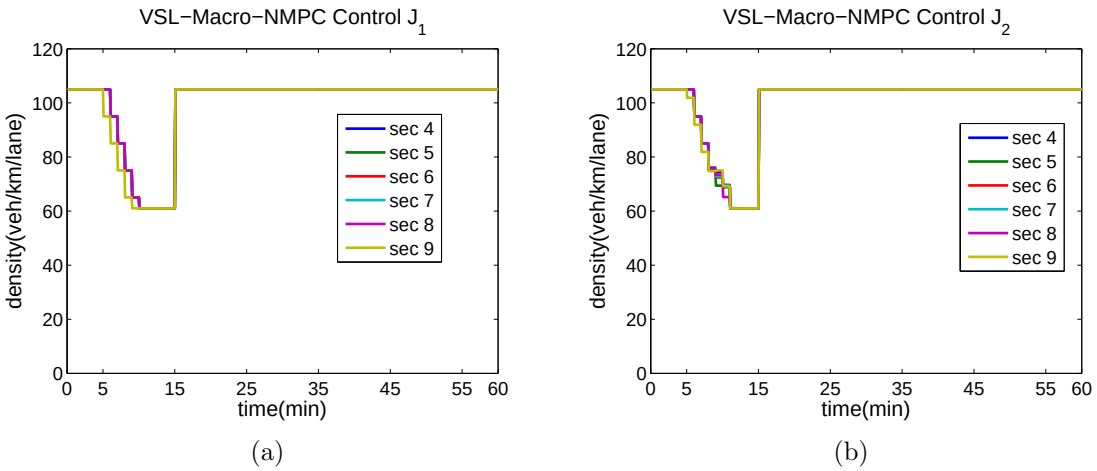

(a) (b)

Figure 3.10: Macroscopic simulation VSL commands: (a) NMPC with cost J_1, and (b) NMPC with cost J_2.

modified according to the characteristics of mainline traffic flow. Ramp metering is usually active when the mainline traffic volume is high. Therefore, the fixed chosen desired occupancy (density) make sense. On the other hand, dynamic variable speed limit is only necessary when disturbance happens, such as accidents. With different disturbance scenarios, traffic volume, and freeway geometry, the desired density is different and usually is difficult to predict. Therefore, we propose a simple proportional speed controller which responses to the changes in downstream density instead of a fixed desired density. Assume we have a freeway segment which is divided into N sections, as shown in Figure 2.1, there is an accident happened

in the most downstream section, section $N+1$, the speed controller of M sections that upstream of section $N+1$ would be active and response to their downstream density changes, as below,

$$V_{min} \leq V_{R,i}(k) \leq V_{max} \tag{3.13}$$

$$\begin{aligned} \bar{V}_{R,i}(k) &= V_{R,i}(k-1) \\ &\quad + K_v[\sum_{j=i+1}^{N+1} \rho_j(k-1) - \sum_{j=i+1}^{N+1} \rho_j(k)] \end{aligned} \tag{3.14}$$

where $V_{R,i}(k)$ is the speed commands of section i; V_{max} is the maximum speed limit allowed, which is often set to be the default speed limit; and V_{min} is the lowest dynamic speed limit we want to apply; K_v is the positive proportional gain. $\bar{V}_{R,i}$ generated by (3.14) may lead to unsafe changes of speed limits. For practical purposes, we use the following speed limit V_i which is smoother.

$$V_{R,i}(k) = \begin{cases} V_{R,i}(k-1) - C_v, & \\ & \text{if } \bar{V}_{R,i}(k) \leq V_{R,i}(k) - C_v \\ V_{R,i}(k-1) + C_v, & \\ & \text{if } \bar{V}_{R,i}(k) \geq V_{R,i}(k) + C_v \\ \bar{V}_{R,i}(k), & \text{otherwise.} \end{cases} \tag{3.15}$$

where C_v is a positive constant represented the biggest changes of speed commands allowed. In this study, $C_v = 10\ km/h$.

3.3.2 Macroscopic Simulation

To demonstrate that this simple controller works as well as the complicated MPC, the benchmark problem in [13] is reproduced with the exact network, traffic scenario, and parameters. In [13], with the MPC proposed, an improvement of 20.1% on TTS is achieved. In this study, we used a very similar downstream density (shown in Figure 3.12) since the original downstream density curve in [13] was described in a figure. The TTS for the no control case is 1754.6 hours, compared to 1853.3 hours in [13]. The TTS for MPC is 1406.9 hours, compared to 1466.7 hours in [13], which is an improvement of 19.8%. The TTS for the proportional controller is 1425.0 hours, which is an improvement of 18.8%. Based on the only quantitative performance measure that macroscopic simulations provided, the proportional controller works as well as the complicated MPC using the macroscopic model used in [13]. Figure 3.13, Figure 3.14 and Figure 3.15 show the density contours of the no control case, MPC case, and proportional controller case, respectively. It is clear that both controller are able to suppress shock waves for this benchmark problem.

3.4 Lane Changing Control

In addition to variable speed limit control, to further regulate traffic flow in case of lane closure, lane change control is shown to be useful to improve safety. Few previous research papers have recognized and studied the lane control problem. [33] developed a microscopic simulation model to evaluate safety impacts of reduced speed zones due to freeway construction/repair activities at different levels of driver compliance. [23] applied a macroscopic simulation model to analyze lane closure strategies for planned work zone. [30] used ALINEA ramp metering operation to manage merging traffic at toll plazas or work zones. Those studies have been focus on relatively permanent merging or lane closure strategies for freeway work zones or other freeway merging sections. Fewer previous research papers have studied

lane control signals for incident management purpose. [36] evaluated the affect of driver compliance rates on the effectiveness of overhead lane control signals. The lane control signals are placed at 1/2 mile intervals and two signals (red "X" symbols) ahead of the incident location were used to show the lane closure. A microscopic simulation model constructed using SLAM (Simulation language for Alternative Modeling) was used to evaluate delay as a measure of performance. [16] used microscopic simulator MITSIM to study three designs of lane control signal settings for the tunnel section of I-93 South. Different number of red and yellow lane control signals within 600 meters ahead of the incident location were applied to two cases with different level of driver compliance rates. The study evaluate travel times for different origin and destination pairs and concluded that not carefully configured lane control signals may result in an increase in the overall travel time, because the trade off between capacity underutilization and smooth lane changing, the sensitivity to the geometrical configuration upstream of the incident and to the driver compliance rate.

While several aspects of the lane control problem have been discussed in those research papers, the main focus was the effectiveness of overhead yellow and red signals on improving travel times. As concluded in [16], lane control signals cause capacity underutilization but give rise to efficient lane changing. The use of lane change guidance will not guarantee travel time reduction but will protect vehicles from sudden and frequent stops on freeways. In this report, we presents and discusses the results and implications of an empirical study on the design and impact of some lane control strategies on resulting traffic patterns in the case of freeway lane closures.

Lane change guidance system is to provide incident and lane blockage information to drivers upstream of the incident location. For example, an incident that takes place at the 8th mile of the freeway segment which can be cleared in five minutes say, blocks one lane and generates shock waves whose effect on congestion

may lasts much longer than five minutes. Upstream vehicles are unaware of the incident. Before the queue developed, those vehicles in the blocked lane keep moving till they could see the accident,reach to a complete stop and have to wait to change to other lanes. After shock waves spread to more lanes upstream, vehicles in all lanes start to blindly change lanes since they do not know if there are lanes blocked and which lanes are blocked. Those blind lane changes create more stops and increase emissions and the possibility of secondary incidents. With vehicle to roadside communication equipped, the incident detection process could be instant. Once an incident is detected, lane change guidance system issue incident warning and lane change guidance to upstream vehicles through roadside to vehicle communication. Information, such as "Incident: lane 3 1000 meters ahead;Estimated lane blockage:10min; Advice: change to lane 1 and 2", guides vehicles in lane 3 to prepare lane change and inform vehicles in the other lanes about the location so they could make their choices and probably reduce the rubber-neck effect. The proposed lane change guidance system could also be implemented in the available overhead signal setting. Red, yellow "X" symbols and arrows could be used to give drivers information about lane blockage and lane change advice except the exact location of the incident.

The design of lane change guidance is a microscopic level control problem. Many elements have been mentioned in [16] to be influential to the outcome of the system, such as how long upstream of the incident the information need to reach, how often the information need to be sent, demanding flow, freeway geometry,and driver compliance rates. Therefore, no analytical method could be used to design the strategies. Microscopic simulations are the best design method available. In this report, we used microscopic simulator VISSIM to facilitate to design a set of lane change guidance strategies with different levels of demanding flow and different incident scenarios for a 6 km long benchmark freeway segment. The average number of stops per vehicle and the average speed from simulation results are used as

performance measures to evaluate the effectiveness of the lane change guidance system.

3.4.1 Benchmark Roadway Network and VISSIM model

Benchmark network is a unidirectional 6 km long 5-lane freeway stretch which is subdivided into 12 sections for the purpose of control. Each section is 500m long and there is an on ramp in section 9. This freeway model is constructed in VISSIM. Parameters using VISSIM are validated using field data from the Berkeley Highway Lab. Details about the validation process could be found in [7]. Since VISSIM is incapable of generating incidents, we use a bus stop to model the incident where a bus will stop in lane 3 at 300m of section 10 for a certain amount of time in order to generate a one lane blockage. Considering the several influential factors of the lane change guidance system, we create four incident scenarios. First, according to the duration of the incidents, we have a 10min incident and a 30min incident. Second, according to the location of the incidents, we have incident downstream of the on ramp and incident upstream of the on ramp (in this case, it is almost equivalent to incident with no ramp flows, therefore, we model this case with zero on ramp flows instead moving the bus stop for modeling simplicity). The effect of on ramps is more critical than that of off ramps because the off ramps will reduce the demanding flow. These four incident scenarios are representative and the same modeling and design methods could be generalized to other scenarios. The function "direction decision" in VISSIM is used to model the lane control. A "Direction decision" only affect a single lane which is what we want for lane control. By assigning the percentage of the vehicles that follow the direction decision, different driver compliance rates could be modeled. The vehicles that have taken the lane change order would just continue if they cannot find a gap to merge which is close to reality and won't generate extra stops. In the beginning of every section, vehicles passing by the control point take commands/information sent by the remote highway traffic

management center (HTMC). One example of the lane change guidance is showing in Figure 3.16. Three sets of lane control commands are activated approximately up to 1.5 km upstream of the incident to guide lane 3 vehicles to change lanes to their left to avoid both on ramp merging area and incident lane. Vehicles in lane 4 and 5 are advised to keep their lanes. Vehicles in lane 1 and 2 are not restricted to change lanes because the on ramp merging. If those vehicles do change to lane 3, they will be guided to change lanes to lane 4 and 5.

3.4.2 Experiments Design

The following variables are key elements to be influential to the effectiveness of the lane change controller.

- Freeway geometry
- Demanding flow rates
- Incident location
- Duration of incidents
- Number of blocked lanes
- Driver compliance rate

Among them, freeway geometry and demanding flow rate represent the conditions of the roadway; incident location, duration and number of blocked lanes represent the nature of the incident; and the driver compliance rates represent the characteristics of the travelers.

With fixed spacing of lane control signals, such as overhead signals or communication points, the following variable we could adjust to improve performance:

- Number of sections controlled

Table 3.2: Scenario information for lane change control

Demanding flow	Low: 1600veh/h/lane for mainline and 100veh/h/lane for on ramp
	High: 1800veh/h/lane for mainline and 500veh/h/lane for on ramp
Incident location	Downstream of on ramp: 300m of section 10
	Upstream of on ramp
Incident duration	10min
	30min
Driver compliance rate	About 80%
	About 20%

- Controller active time

Furthermore, we could probably swing driver compliance rates by sending the right information. For example, for overhead signals, if we want higher compliance rate, we could display more red signals instead of yellow signals.

In this study, we use the benchmark network as an example and we set the bus to stop in lane 3 all the time. Therefore, the freeway geometry and number of blocked lanes are fixed. We create sixteen scenarios corresponding to four factors each with two levels. Table 3.2 shows detailed information for the sixteen scenarios. We conduct one-hour-long simulation runs for the sixteen scenarios for three cases: w/o incident w/o lane change guidance (LCG); w/ incident w/o LCG; and w/ incident w/ LCG to compare the performance measures. The two performance measures: number of stops per vehicle and averaged speed, are used as feedback to tune the number of sections under control and controller active time. These sixteen scenarios are typical examples of possible scenarios for one lane blockage. In general, for a certain freeway geometry, the tuned sixteen controllers corresponding to the sixteen scenarios could be saved in database and one of them could be activated based on the real time traffic and incident surveillance information.

Table 3.3: Lane change control simulation results (1)

	10 min Incident, downstream of the on ramp					
	Low Inflow (1600, 100)			High Inflow (1800, 500)		
	Number of Stops Per Vehicle	Change	Average speed [km/h]	Number of Stops Per Vehicle	Change	Average speed [km/h]
W/O Incident W/O LCG	0	-	105	0	-	103
W/ Incident W/O LCG	0.038	-	104	0.35	-	95
W/ Incident W/ LCG						
80% compliance rate	0.018	-53%	104	0.272	-22%	96
20% compliance rate	0.055	45%	104	0.397	13%	95

3.4.3 Simulation Results

Figure 3.17 shows the lane controller designed for the scenario with 10min incident downstream of the on ramp, high demanding flow rate and 80% driver compliance rate. There are lane control signals up to 4 sections upstream of the incident and they are active during the whole 10min while lane 3 is blocked. Because of the high demanding flow merging from the on ramp in section 9, the lane change guidance for section 7, 8, and 9 include commands for lane 3 vehicles to change to the left and for lane 4 and 5 vehicles to keep their lanes. Table 3.3 shows the two performance measures for the above controller compared with no incident no control case and with incident no control case. The demanding flow rates (1800 veh/h/lane for mainline and 500 veh/h/lane for the on ramp) are very close to the capacity. Without any incidents, no vehicles need to stop. The incident cause every vehicle to stop 0.35 times on average without control. The lane change controller reduces the number of stops by 22% with slightly increased average speed.

Also shown in Table 3.3, for the 20% compliance rate, lane change control actually increases the number of stops while maintain a relatively consistent average speed. In the case of short time lane block, the controller's disturbance effect overtakes its smoothing effect if most of the drivers do not comply.

Table 3.4: Lane change control simulation results (2)

	30 min Incident, downstream of the on ramp					
	Low Inflow (1600, 100)			High Inflow (1800, 500)		
	Number of Stops Per Vehicle	Change	Average speed [km/h]	Number of Stops Per Vehicle	Change	Average speed [km/h]
W/O Incident W/O LCG	0	-	105	0	-	103
W/ Incident W/O LCG	0.278	-	99	5.843	-	60
W/ Incident W/ LCG						
80% compliance rate	0.467	68%	96	5.861	0%	60
20% compliance rate	0.63	127%	96	5.542	-5%	60

Table 3.4 is showing the simulation results for 30min incident downstream of the on ramp. The results for the other eight scenarios are similar to the shown ones therefore omitted. It is interesting to notice that there are almost no positive effects on either number of stops or average speed when the incident lasts much longer and the controllers are active as long as the lane is blocked. Queues will spread to all the lanes and several sections upstream of the incident location if the incident lasts long enough. Once traffic has transited to the complete congested state, there is no longer room for any controllers to work.

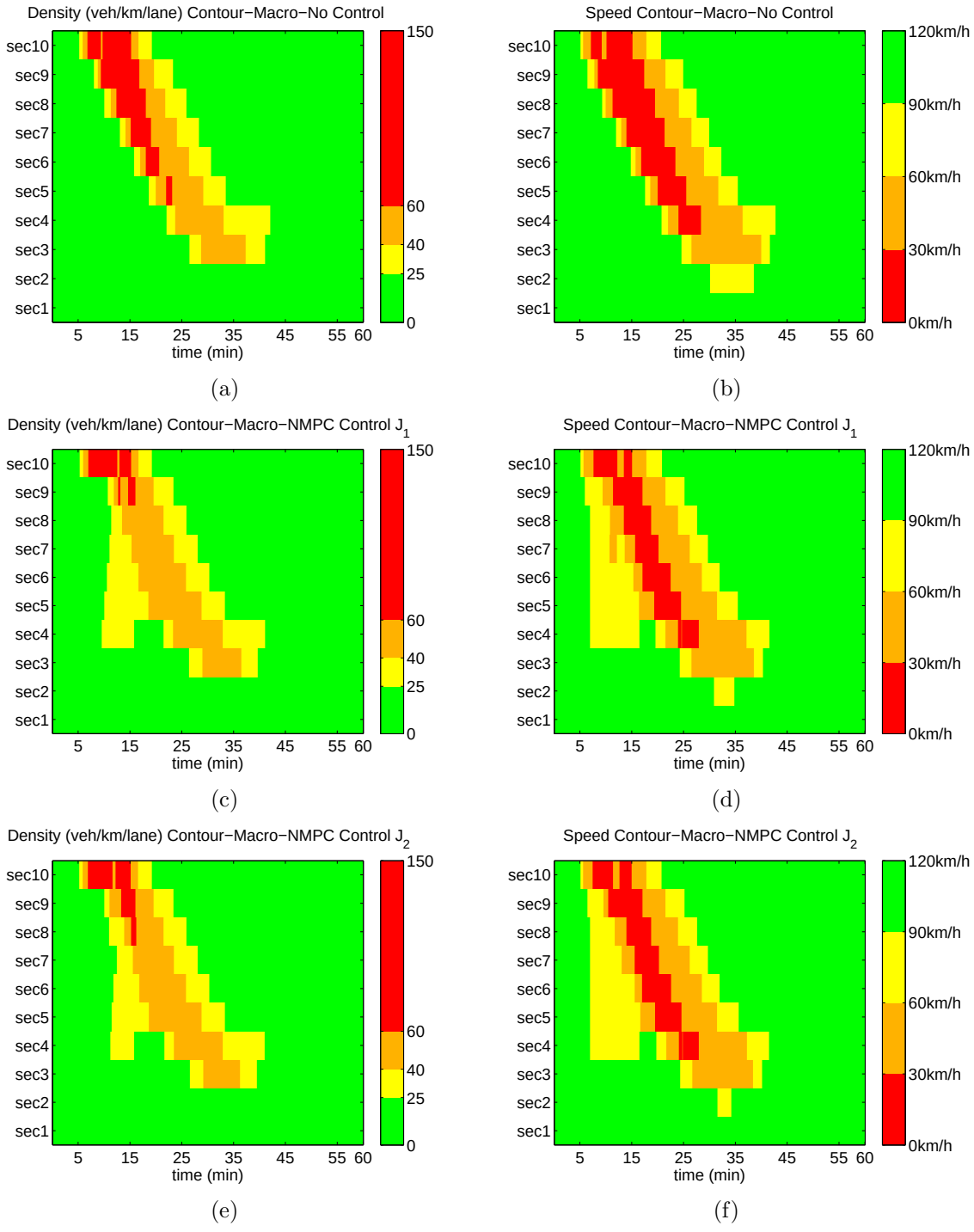

Figure 3.11: Macroscopic simulation: No control (a) density contour, (b) speed contour, and NMPC cost J_1 (c) density contour,(d) speed contour, and NMPC with cost J_2 (e) density contour,(f) speed contour.

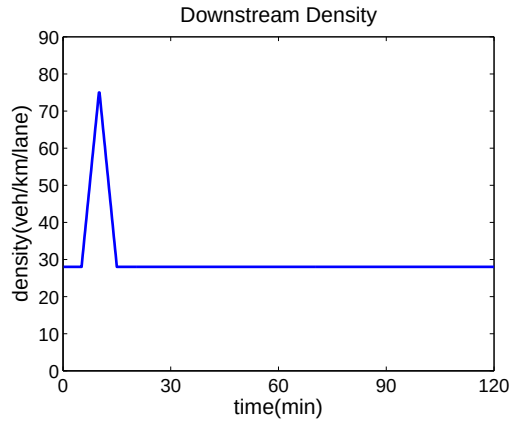

Figure 3.12: Density curves of section N+1

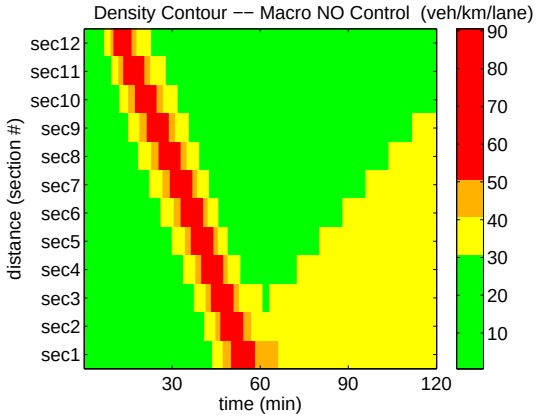

Figure 3.13: Density contour without control

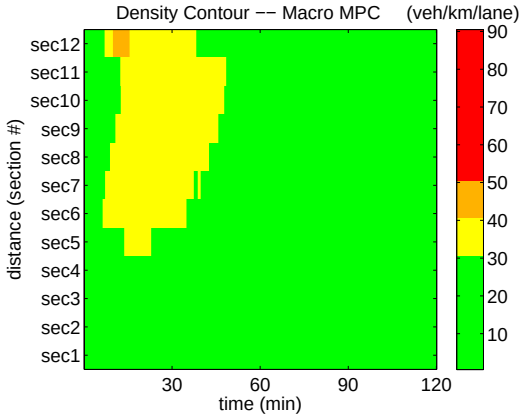

Figure 3.14: Density contour with MPC

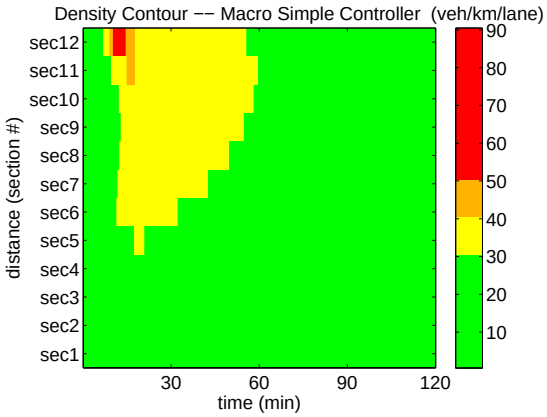

Figure 3.15: Density contour with simple controller

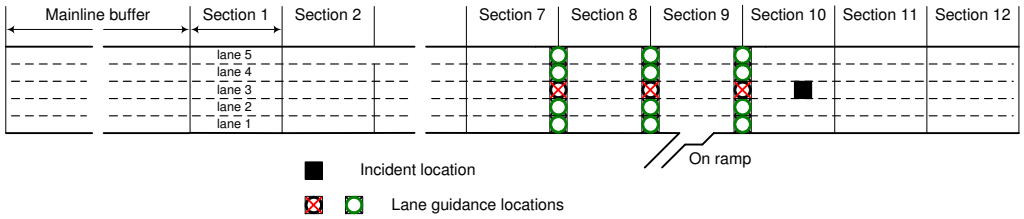

Figure 3.16: The benchmark network for lane change control

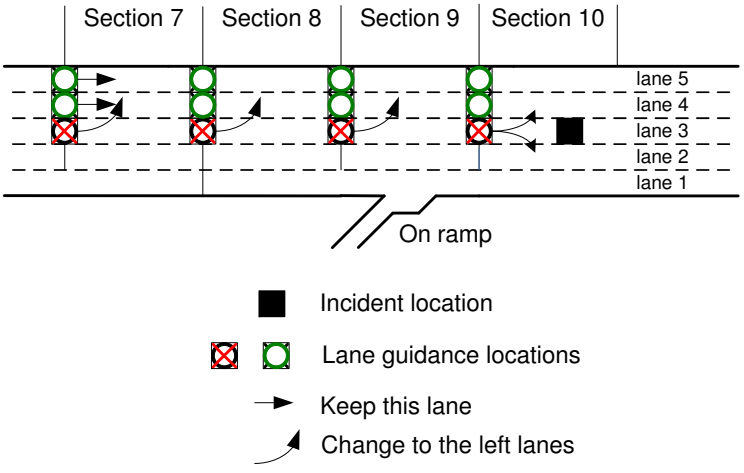

Figure 3.17: Lane chang controller designed for 10min incident,high demanding flow and high compliance rate.

Chapter 4

Performance Evaluation

4.1 VISSIM Model

Since actual experiments involving new traffic flow control algorithms are not desirable due to cost and possible adverse effects on traffic, extensive simulation studies need to be performed to evaluate the performance and robustness of the proposed VSL control systems before an actual demonstration.

Simulation models could assist transportation engineers in evaluating alternative transportation strategies and in predicting outcomes of an improvement of the transportation systems. Traffic simulation models can generally be classified into macroscopic and microscopic models. Macroscopic simulation models are deterministic relationships of aggregated variables, flow, speed, and density of the traffic stream. Microscopic models, on the other hand, simulate the individual vehicle movements based on car-following and lane-changing theories and could be stochastic or deterministic. Since macroscopic models do not describe the traffic on the level of individual vehicles, they are less computationally intensive. They also have fewer parameters to calibrate than microscopic models. However, macroscopic models are sometimes not sufficient to capture the desired level of details and some phenomena of traffic. Recently, microscopic models have increased their area of application since more computing power is available. Accordingly, microscopic models

are effective in the operation of complex transportation systems and the investigation of ITS (Intelligent Transportation System) where a greater level of details is required. Some of the popular microscopic simulators for freeway systems are VISSIM (PTV, Germany), Aimsun (TSS, Spain),Paramics(Quadstone Inc, Scotland), CORSIM (FHWA, U.S.), and TransModeler(Caliper, U.S.).

VISSIM is a stochastic microscopic traffic simulator which uses the psycho-physical Wiedemann [41, 42] car following model and powerful lane-changing behavior models with realistic modeling of various merging situations. It provides a COM (component object model) programming interface so users could integrate VISSIM in their own applications using languages like Visual Basic or C++ to access the network topology, signal control and other data on-line. With high level of details, VISSIM is an ideal tool to simulate different traffic scenarios before starting implementation of certain traffic control strategy.

4.1.1 Network Modeling

To build a VISSIM model, the first step is to draw the roadway map in the form of links and connectors (Figure 4.1 shows an example of a roadway network model in VISSIM)and specify the parameters, such as link length and number of lanes. The second step is to set base data such as acceleration and deceleration functions, desired speed distributions and other vehicle distributions, vehicle type, vehicle composition, and routes. Moreover, car following parameters, vehicle inputs and controls need to set up which are described in details in the following sub sections.

4.1.2 Car Following Model

VISSIM is a discrete time step based (for example, in this study, time step is 0.2 second) microscopic traffic flow simulation model including the car following and lane change logic. VISSIM uses the psycho-physical driver behavior model developed by WIEDEMANN ([41]).The basic concept of this model is that the

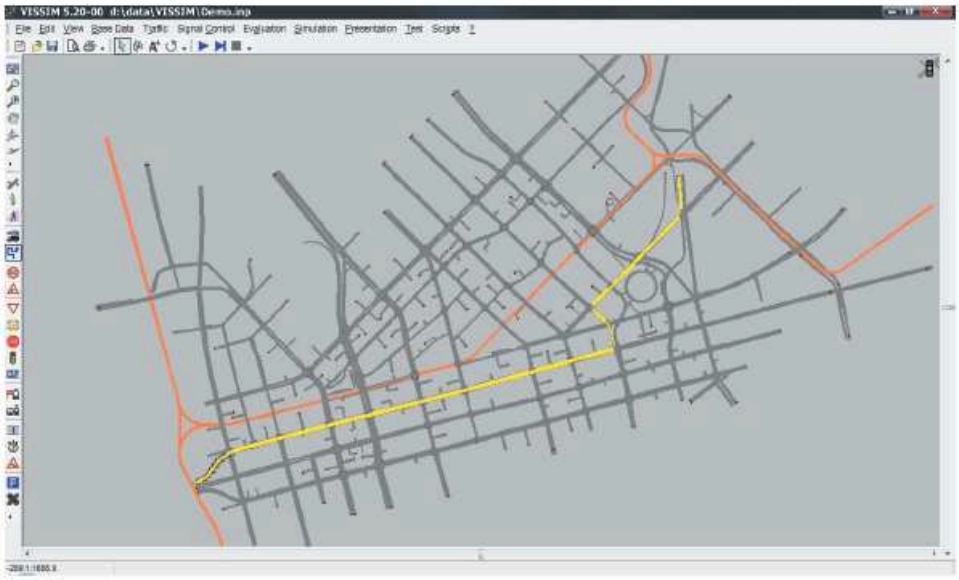

Figure 4.1: A screen shot of VISSIM

driver of a faster moving vehicle starts to decelerate as he reaches his individual perception threshold to a slower moving vehicle. Since he cannot exactly determine the speed of that vehicle, his speed will fall below that vehicles speed until he starts to slightly accelerate again after reaching another perception threshold. This results in an iterative process of acceleration and deceleration. Stochastic distributions of speed and spacing thresholds are used to replicate individual driver behavior characteristics. The accuracy of this traffic simulator is hence improved over other less complex models which use constant speeds and deterministic car following logic.

4.1.3 Stochastic Modeling

VISSIM is a stochastic simulator. First of all, users could specify the CDFs (Cumulative Distribution Function) of the parameters of the car following model. Secondly, instead of a single acceleration or deceleration value, VISSIM uses functions

to represent the differences in a driver's behavior. These acceleration and deceleration functions have the minimum, mean and maximum value curves to reflect the stochastic distribution. Thirdly, CDFs of desired speeds are defined for each vehicle type. A lot of other parameters, such as vehicle weight, powder and model follow user specified CDFs too. In light of the stochastic nature of VISSIM simulator, Monte Carlo method is used to get a good impression of the possible stochastic spread of results. VISSIM uses a parameter 'Random Seed' to initialize the random number generator. In this study, multiple simulation runs (usually 10-20) with different random seeds are conducted for every case.

4.1.4 Simulation Inputs and Outputs

Demand in terms of flow rate is modeled through "Vehicle Inputs" in VISSIM. In macroscopic simulations,if demand at section 1 (the most upstream section) can not be met, vehicles will wait in the virtual link outside the network. In reality, this is impossible. Shock waves will propagate back until they are absorbed. There are no virtual parking lot on the freeway so that vehicles travel at free flow speed and suddenly stop to wait. To model this reality, a several km long buffer is added to the upstream of the considered freeway segment. This buffer is designed to absorb the shock waves and to make sure that the demand to the network is met all the time. When evaluate the performance, vehicle travel time in this buffer is also counted which reflect the effect of VSL (the second rate shock waves) to the upstream of the controlled area. While in macroscopic simulations, only the waiting time of these vehicles are considered. The second rate shock wave effect is omitted.

VISSIM simulation generates an online visualization of traffic operations and offline output files gathering data such as vehicle trajectories, total travel time, total travel distance, total stops, total lane changes number, time series of space averaged speed, time series of flow measured at fixed locations, time series of link density, and so on.

4.1.5 Bottleneck Modeling

In macroscopic simulation, a bottleneck sometimes is modeled with a fixed downstream density curve which has high density during a certain duration of time ([13]). In microscopic simulations, a recurrent bottleneck is either a physical lane drop, a diverge or a merge; and a nonrecurrent bottleneck could be an accident causing lane closure or a slow moving vehicle. In this study, we focus on nonrecurrent bottleneck, i.e., the accident case. VISSIM has disadvantages in modeling merging scenario since some vehicles could be drop while waiting to merge. In this study, we used two methods to model an accident. First, a lane closure is implemented by VISSIM's own lane closure function. Second, a very slow moving bus is created to model a moving bottleneck. For example, a bus is created at the beginning of the most downstream section to move at 5km/h. If the section is 1km long, this bus would block a lane for about 10min hence mimic an accident caused lane closure for 10min.

4.1.6 VSL Modeling

In VISSIM, there are two ways to model desired speed changes, one is "Reduced Speed Areas" and the other one is "Desired Speed Decisions". The main difference between the two is, that with reduced speed areas a (faster) vehicle automatically decelerates prior to the start of the reduced speed area to get the desired speed of the "reduced speed area" right at the start of it. After passing the reduced speed area the vehicle automatically accelerates to the desired speed that previously was assigned to it. While in the "Desired Speed Decisions" case, a vehicle is affected when passing the decision point. In this study, the "Desired Speed Decision" method is used to model the overhead speed limit signs. The desired speed distribution is assigned by the user by a min speed and a max speed. In this study, two sets of "Desired Speed Distribution" were used and list in Table 4.1.When entering the network, each vehicle gets a fixed percentile value for speed distribution.

Table 4.1: Desired Speed Distribution Tables for VISSIM Models

DSD type I				DSD type II		
Desired Speed (km/h)	Min (km/h)	Max (km/h)		Desired Speed (km/h)	Min (km/h)	Max (km/h)
50	48	58		50	50	51
55	53	63		51	51	52
60	58	68		52	52	53
65	63	73		.....		
70	68	78				
75	73	85				
80	75	110				
85	80	115				
90	85	120				
95	86	125		103	103	104
100	88	130		104	104	105
105	90	135		105	105	106

For example, if vehicle NO.10 gets the number 40%, then vehicle NO.10 will always get the 40% percentile of the desired speed distribution at desired speed changes. If vehicle NO.10 gets 100%, then it will always get the maximum speed value of that distribution. In Table 4.1,type I DSD has a difference of 10km/h between the minimum and the maximum speeds, which means that vehicles pass this type of DSD points possibly to get any desired speed limit between the min and max values depending on the percentile number assigned to them. On the other hand, type II DSD only has a freedom of 1km/h. Vehicles will follow the almost exact desired speed when pass this type of DSD points.

The locations of the VSL signs and the frequency they appear are also problems of modeling and implementations. In this study, several spacings of the DSD points are used and the details are presented with the introduction of each of the simulation cases.

4.1.7 Model Validation

Car-following model is the fundamental element of a microscopic model and its parameters need to be calibrated against field data. Inductive loop detector data from the Berkeley Highway Laboratory (BHL) which is a stretch of the Interstate-80, immediately east of the San Francisco-Oakland Bay Bridge are used to tune and calibrate a VISSIM BHL model so that it accurately represents the traffic flow characteristics. Calibration process is explained in detail in [39].

4.2 Integrated Simulation/Evaluation Framework

To get on-line measurements from VISSIM, calculate VSL commands using the controllers, and apply commands to VISSIM in real time, an integrated framework is developed. VISSIM provides a COM interface to allow user applications to access network objects, such as a "lane" object to close it for a period of time, a "desired speed decision" object to implement the VSL command, and "link" objects to get real time link speed and density measurements at the sampling time. The MATLAB engine library contains routines that allow users to call MATLAB software from users' own programs, thereby employing MATLAB as a computation engine. The engine library is part of the MATLAB C/C++ and Fortran API (application programming interface) Reference. It contains routines for controlling the computation engine. As shown in Figure 4.2, an external C++ program is written to access VISSIM COM interface and communicate data between the controller which is implemented in MATLAB and VISSIM in real time.

4.3 Simulation Results

Using the integrated simulation framework (Figure 4.2), 3 different freeway network with several traffic scenarios were studied and details are presented below.

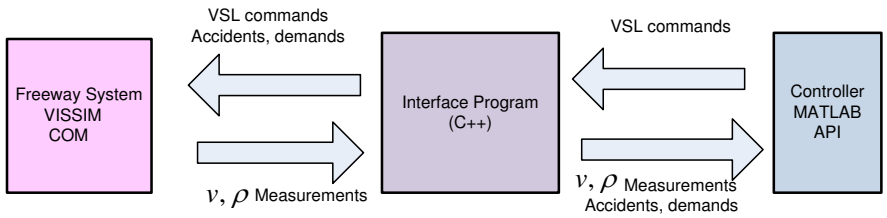

Figure 4.2: Integrated framework to test VSL control system

4.3.1 Performance Measures

To evaluate possible benefits of VSL control in mobility and environmental quality, several performance measures which are available from VISSIM simulation runs are chosen. For mobility, they are total travel time (of all vehicles pass the freeway segment during the simulation run), average speed, and travel cost in terms of fuel consumption. For environmental impact, they are tailpipe emissions, such as carbon dioxide (CO2), hydrocarbons(HC), nitrogen oxides (NOx) and carbon monoxide(CO). Moreover, two indirect measures of traffic flow smoothness and safety, the average number of stops (per vehicle) and the average number of lane changes (per vehicle) are also included. Excepts the fuel consumption and tailpipe emissions, the other variables are directly measured by VISSIM. To estimate fuel consumption and tailpipe emissions, we adopt the Comprehensive Modal Emissions Model (CMEM) developed by a research group at UC Riverside [4]. CMEM takes speed and acceleration profile of every vehicle sampled every second which are available from VISSIM as inputs, calculate engine speed and engine power, and hence estimate fuel rate and tailpipe emissions.

4.3.2 Network I

Network I is the same freeway segment used in section 3.1 and section 3.2. The only difference is that this VISSIM model is 7km long instead 5km in the macroscopic model. A 2-km buffer was added upstream of section 1 to make it more realistic. In

macroscopic simulations, if demand at section 1 can not be met, vehicles will wait in the virtual link outside the network. In reality, this is impossible. Shock waves will propagate back until they are absorbed. The 2km-long buffer is designed to absorb the shock waves and to make sure that the demand to the network is met all the time. Therefore, Network I is 7-km long freeway segment with 5 lanes. The first 2km is not controlled, and the rest 5km are divided into 10 sections, 500m each. The mainline demand is 1800 veh/h/lane and the accident is modeled by closing 2 lanes (using VISSIM lane closure function) in section 10 for 10 minutes. One simulation run is 90 minutes with the last 15 minutes without any vehicle inputs to clear out the network so every simulation run will have the same total number of vehicles and Total Distance Traveled (TDT) to facilitate comparison. Three controllers described in section 3.1 and section 3.2, the virtual mainline metering/simple VSL controller, the NMPC with cost J_1, and the NMPC cost J_2 are evaluated.

The VSLs are implemented in two different ways. First, the Desired Speed Decision (DSD) points are placed at the beginning of each section, i.e., 500 meters apart. Once a vehicle passes this DSD point, it takes the new speed limit and start to decelerate according to its deceleration function or accelerate if safe according to its acceleration function. In this case, type I DSD is used which models that drivers don't follow the speed limits exactly.

The second type of VSL implementation is to place an extra DSD point in the middle of the section, i.e., the DSDs are 250 meters apart. The controllers calculate the speed commands at the beginning of each section and the DSD in the middle of the section takes the average value between the two adjacent speed commands. This implementation is to model how drivers react to speed limits. Drivers see the speed limit signs several hundreds meters ahead and start to decelerate to reach the speed limit value when they reach the location of the signs.

The performance measurements of the aforementioned three controllers are listed in Table 4.2. The percentage changes in the table are $\frac{(Controlled-NoControl)}{NoControl} X 100\%$.

Since all the measurements are the less the better, if the percentage change is negative, it means the controller improves this performance. Compare to the base case which is the no control case, all three controller improve the smoothness indicated by reduced average number of stops while keep the travel time relatively unchanged. Since the fuel consumption and emission are highly positively correlated with travel time, these two measurements are more or less the same. The results presented in Table 4.2 are from simulations runs with one random seed. Results from Monte Carlo runs are presented in the later sections.

Among the three controller, the simple VSL controller has the biggest improvement which is confirmed by the density and speed measured from the simulations, shown in Figure 4.3, Figure 4.4, Figure 4.5, and Figure 4.6. Shock waves are partially suppressed by the simple VSL controller so that the peak density values are reduced for every section and the minimum speed values are increased for every section. However, if we compare the simulation results of VISSIM simulations and their counterparts from the macroscopic simulations, controllers are less effective in suppressing shock waves hence alleviating congestion although the generated VSL signals are similar (generated VSL signals from VISSIM are shown in Figure 4.7 and Figure 4.8). This shows that due to the fact that macroscopic models are incapable of modeling certain vehicle level dynamics, such as lane changing, the travel time benefits demonstrated by macroscopic simulations in some of the literatures might be over optimistic. Moreover, the simulation results also show that the simple VSL controller that does not rely on any models is not inferior to the more complicated and computation demanding model predictive controllers.

4.4 Monte Carlo Simulation

Traffic flows are stochastic in nature with uncertainty, ambiguity, and variability. Many elements, such as demand, accident severity,freeway geometry and VSL

Table 4.2: Network I VISSIM Simulation Performance Measurements

VSL	Ave Demand (veh/h /lane)	Accident	Total Number of Vehicles	ctrl	TTS (hours)	%	Ave Speed (km/h)	Ave Number of Stops (per vehicle)	%	Ave Lane Change (per vehicle)	%	Ave Fuel (g/km/ veh)	%	Ave CO2 (g/km/ veh)	%
	1800	2 out of 5 lanes closed for 10 min	11250	No Control	990.3		91.1	1.3		4.6		80.2		254.1	
Every 500m				Virtual Mainline Metering	1015.9	2.6	88.8	0.7	-45.7	4.4	-4.3	82.1	2.4	259.9	2.3
				NMPC J1	987.0	-0.3	91.4	1.1	-11.8	4.6	0.0	79.9	-0.4	253.2	-0.4
				NMPC J2	996.8	0.7	90.5	1.1	-15.0	4.5	-2.2	81.0	1.0	256.4	0.9
Every 250m				Virtual Mainline Metering	989.3	-0.1	91.2	0.5	-61.4	4.5	-2.2	79.9	-0.4	253.1	-0.4
				NMPC J1	981.4	-0.9	91.9	1.1	-11.0	4.6	0.0	79.4	-1.0	251.5	-1.0
				NMPC J2	999.2	0.9	90.3	1.1	-11.8	4.4	-4.3	81.0	1.0	256.7	1.0

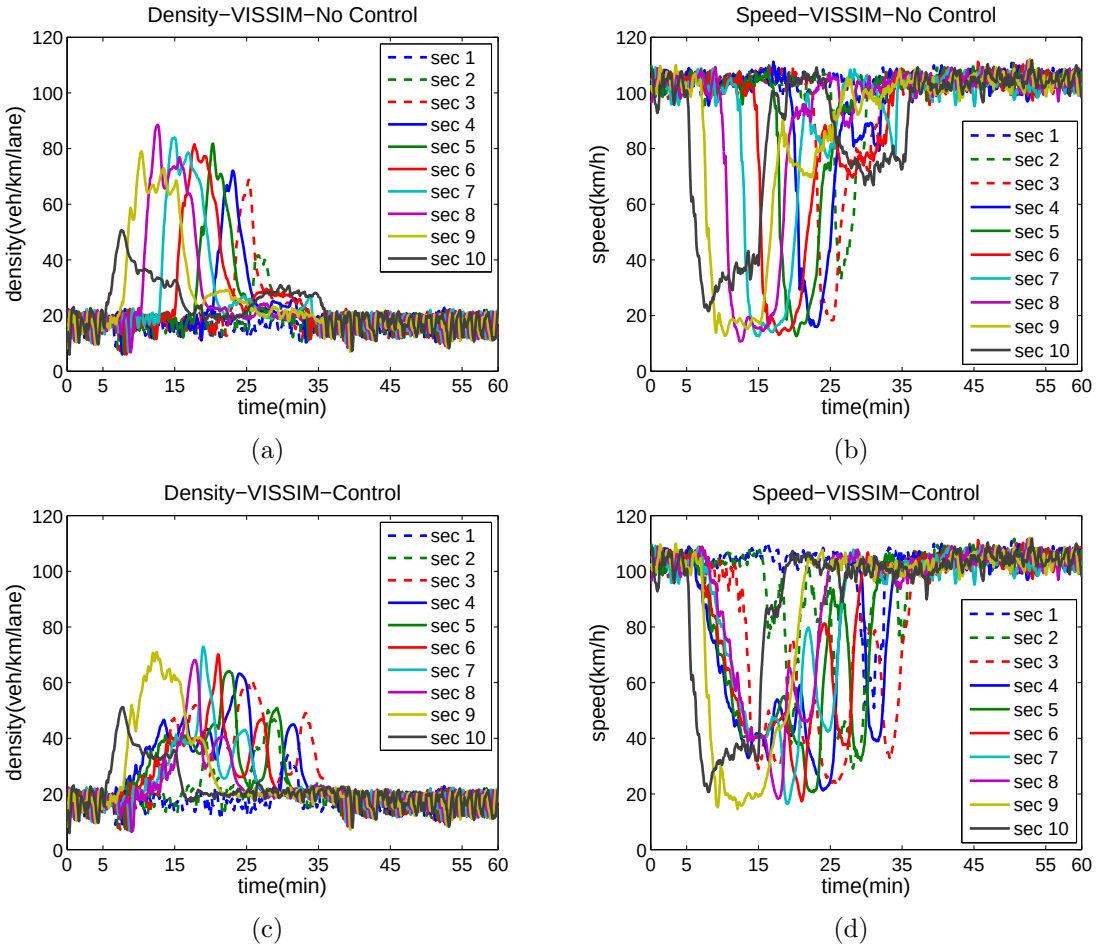

Figure 4.3: VISSIM simulation Network I (1): No control (a) density, (b) speed, Simple controller (c) density, (d) speed.

implementation could have impact on the simulation outcome. To evaluate the proposed controllers to some extent, ten scenarios with different freeway segments, demand levels, accident scenarios, and VSL implementations are studied to take into variability into consideration. These ten scenarios are described in Table 4.3. Many of VISSIM's parameters are not fixed single values but probability distributions. Monte Carlo simulations for each scenario are conducted in order to better assess the impact of uncertainty. The performance measurements are average numbers from at least ten simulation runs with different random seeds for each scenario and each controller.

Table 4.3: VISSIM Simulations Scenario Description

Scenario NO.	Network	Case NO.	Sim Time	Demand	Accident	DSD Type	VSL Spacing
1	**II**. 9km, 5 lanes		150 min	1800 veh/h/lane for 0-135min and zero demand for 135-150min	Two buses, two lanes blocked for 10 min	**I**. 50-105 km/h, every 5km/h	Every 0.5 km
2				1700 veh/h/lane for 0-135min and zero demand for 135-150min			
3				1800 veh/h/lane for 0-135min and zero demand for 135-150min	Three buses, three lanes blocked for 10 min		
4	**III**. 7km 2 lanes	**1**		1900 veh/h/lane for 0-135min and zero demand for 135-150min	One bus, one lane blocked for 10 min	**I**. 50-105 km/h, every 5km/h	Every 1 km
5				1800 veh/h/lane for 0-135min and zero demand for 135-150min			
6				1900 veh/h/lane for 0-135min and zero demand for 135-150min	One bus, one lane blocked for 15 min		
7		**2**		1900 veh/h/lane for 0-60min and 500 veh/h/lane for 60-120min and zeros demand for 120-150min	One bus, one lane blocked for 60 min	**II**. 50-105 km/h, every 1km/h	Every 0.1 km
8				1500 veh/h/lane for 0-60min and 500 veh/h/lane for 60-120min and zeros demand for 120-150min			
9				1000 veh/h/lane for 0-60min and 500 veh/h/lane for 60-120min and zeros demand for 120-150min			
10				500 veh/h/lane for 0-120min and zeros demand for 120-150min			

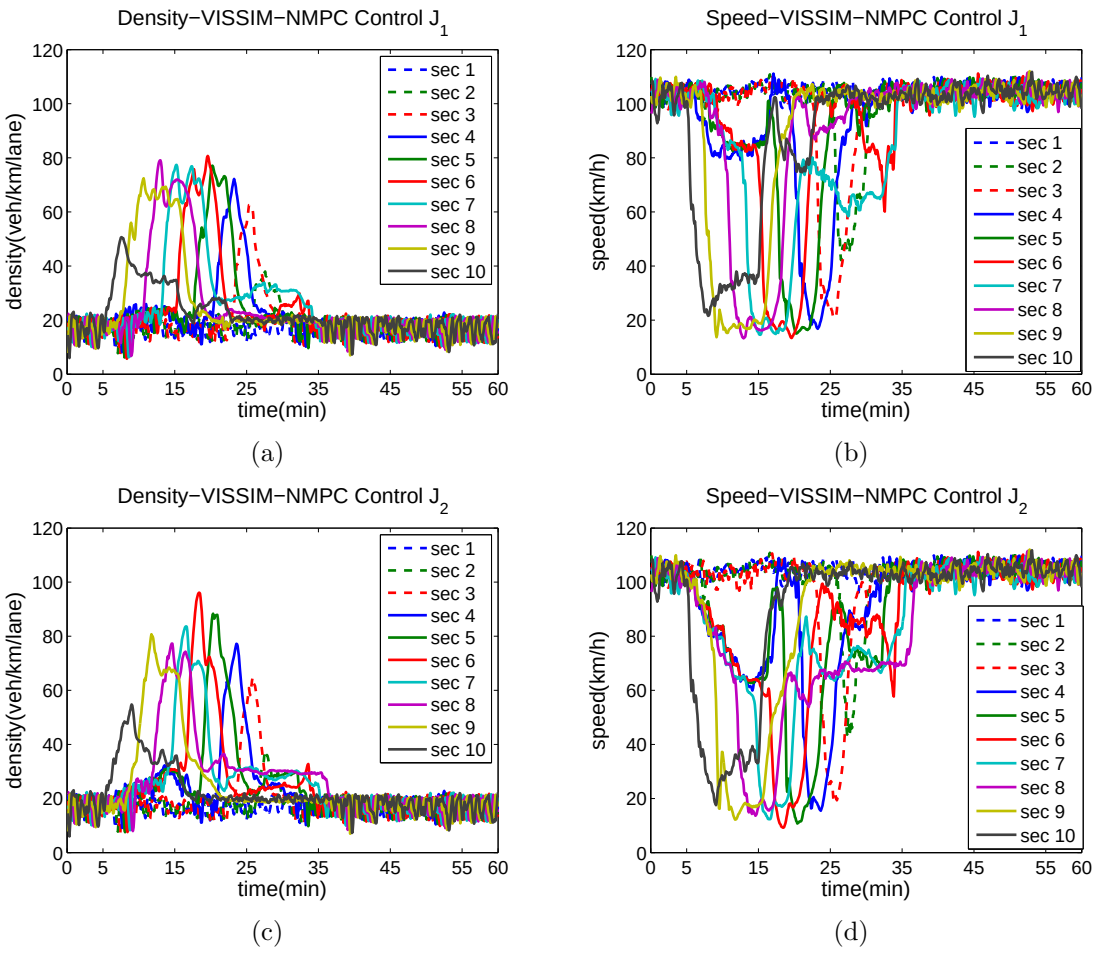

Figure 4.4: VISSIM simulation Network I (2): NMPC with cost J_1 (a) density, (b) speed, NMPC with cost J_2 (c) density, (d) speed.

4.4.1 Network II

Network II is a 9km freeway segment with 5 lanes. It has a 2km long buffer and 14 0.5-km-long sections. The simple controller used in this case is the proportional speed controller presented in section 3.3 and the MPC is the one used in [13] with its parameters calibrated using VISSIM data. The macroscopic version of the Network III simulations are presented in section 3.3.2. The macroscopic simulations show that both of the controllers could reduce TTS by about 20% and suppress shock waves.

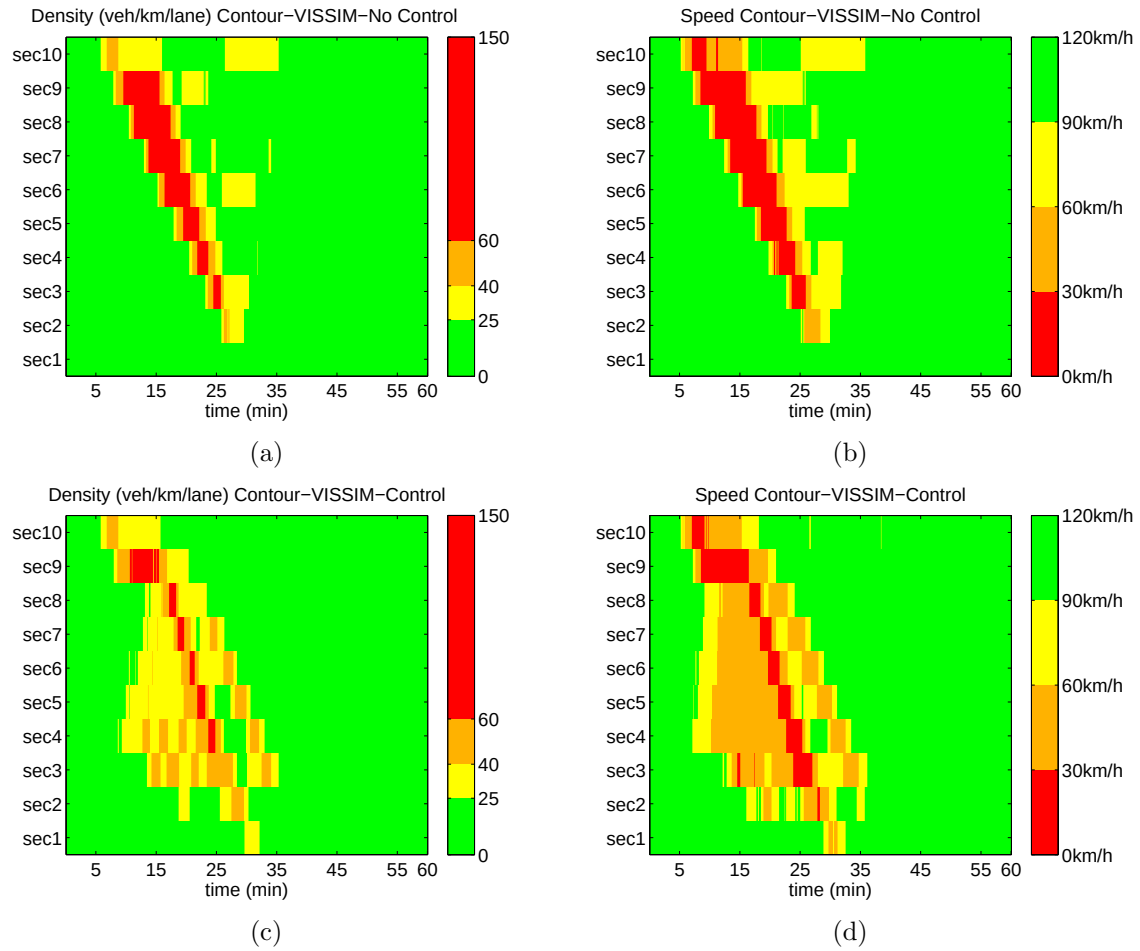

Figure 4.5: VISSIM Simulation Contour Network I (1): No control (a) density contour, (b) speed contour, Simple controller (c) density contour, (d) speed contour.

The mainline demand varies from 1700veh/h/lane to 1800 veh/h/lane. The accident is modeled by several slow moving buses blocking several lanes in the most downstream section. Simulation time is 150 minutes. For every scenario, the case without controller is simulated to be used as baseline. At least 10 runs with different random seeds are conducted for every scenario and every controller (including no control). Desired Speed Decision (DSD) points are type I in Table 4.1 and are spaced every 0.5 km, i.e., one DSD every section.

The performance measurements, i.e., Total Travel Time (TTT), Average Number of Stops (per car), Average Number of Lane Changes (per car), Average Fuel

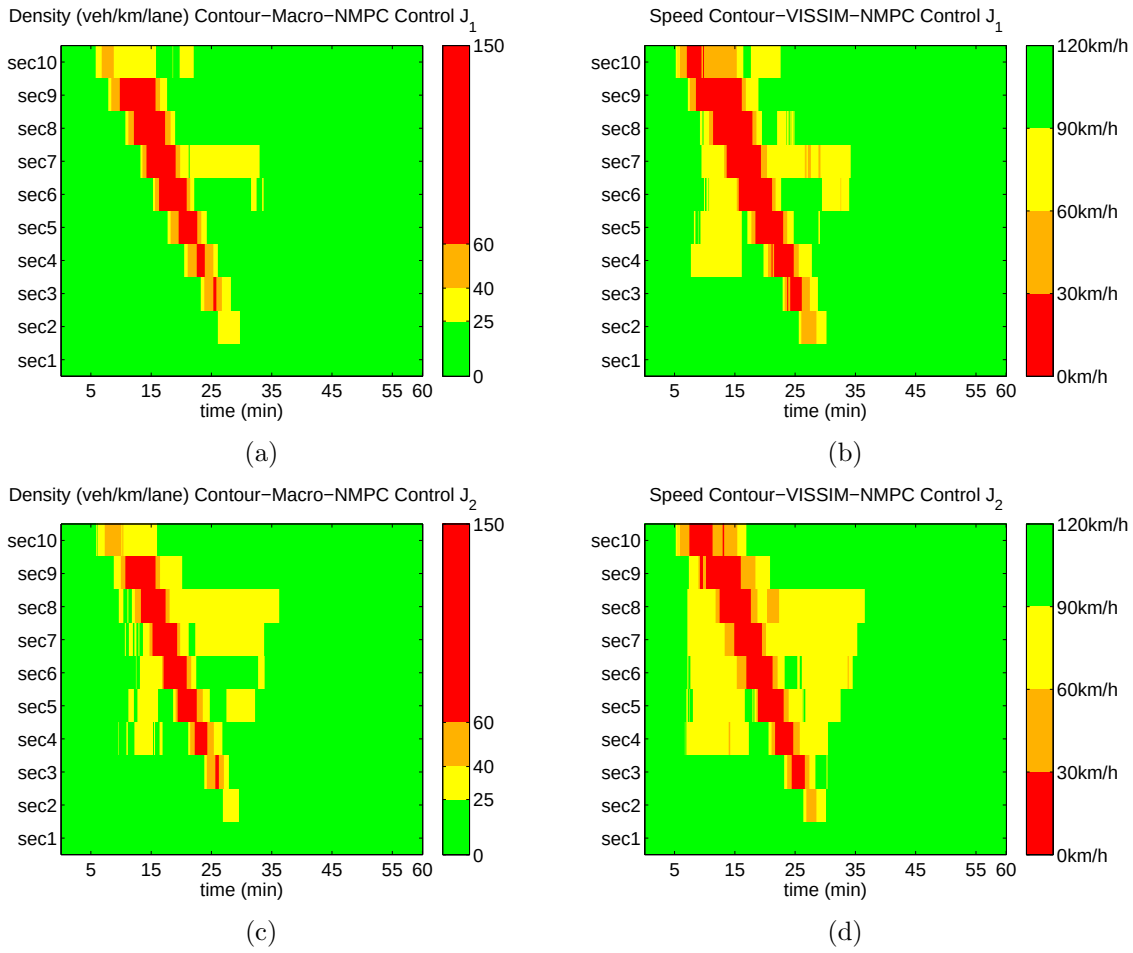

Figure 4.6: VISSIM Simulation Contour Network I (2): NMPC with cost J_1 (a) density contour, (b) speed contour, and NMPC with cost J_2 (c) density contour, (d) speed contour.

Consumption, and Average CO_2 Emission from the three controllers of scenario 1-3 are shown in Figure 4.9 and Table 4.4. Comparing controlled cases to no control cases, TTT is more or less the same, especially for the simple controller. Hence, fuel consumption and tailpipe emissions are more or less the same since they are related to travel time given that the Total Distance Traveled (TDT) is a constant. Safety measurements,such as number of stops are reduced from 20% to 90%, and number of lane changes are reduced consistently.

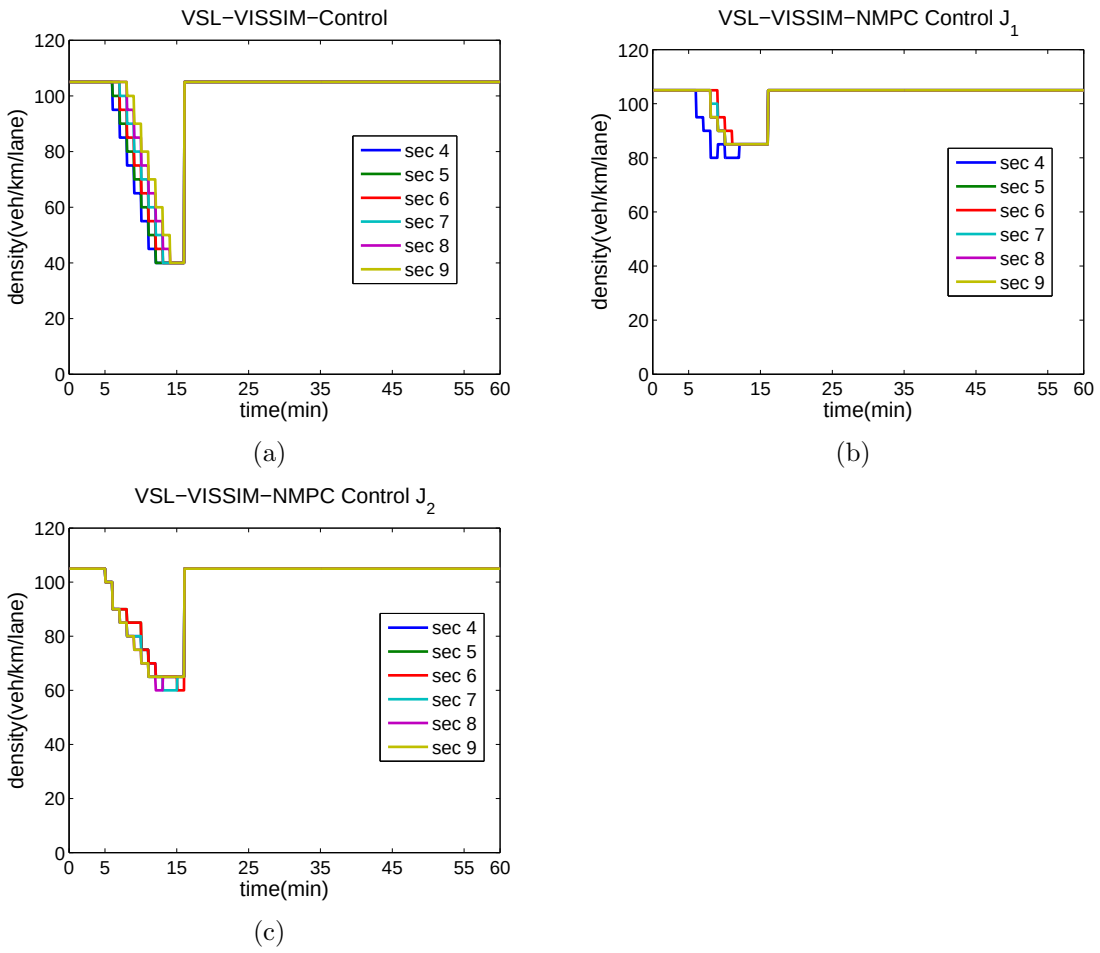

Figure 4.7: VISSIM simulation VSL commands Network I: (a) simple controller,(b) NMPC with cost J_1, and (c) NMPC with cost J_2.

4.4.2 Network III

Network III is a 17km freeway segment with 2 lanes. It has a 4km long buffer and 13 1-km-long sections. The simple controller used in this case is the proportional speed controller presented in section 3.3 and the MPC is the one used in [13] with its parameters calibrated using VISSIM data. The macroscopic version of the Network III simulations are presented in section 3.3.2. The macroscopic simulations show that both of the controllers could reduce TTS by about 20% and suppress shock waves.

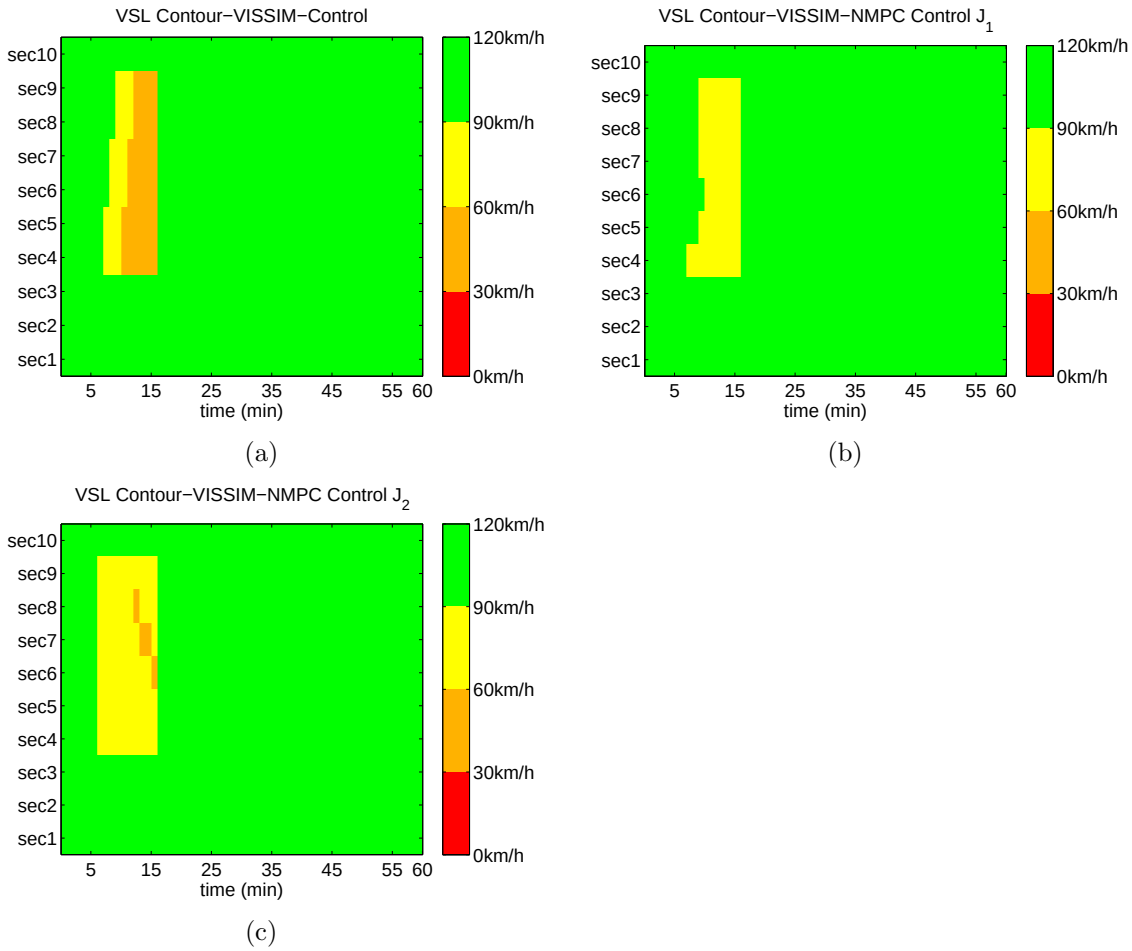

Figure 4.8: VISSIM simulation VSL command contours Network I: (a) simple controller, (b) NMPC with cost J_1, and (c) NMPC with cost J_2.

The mainline demand varies from 500veh/h/lane to 1900 veh/h/lane which is close to the capacity of 2100 veh/h/lane. The accident is modeled by a slow moving bus blocking one lane in the most downstream section. Simulation time is 150 minutes. For every scenario, the case without controller is simulated to be used as baseline. At least 10 runs with different random seeds are conducted for every scenario and every controller (including no control).

The VSLs are implemented in two different ways. For scenario 4-6 in case 1, the Desired Speed Decisions (DSD) are type I in Table 4.1 and are spaced every 1 km. For scenario 7-10 in case 2, DSDs are type II in Table 4.1 and are spaced every 0.1

km. The controllers calculate speed limits for every section/every 1km. The DSDs in between these calculated DSD points are interpolated to model a smoother speed change.

The performance measurements, i.e., Total Travel Time (TTT), Average Number of Stops (per car), Average Number of Lane Changes (per car), Average Fuel Consumption, and Average CO_2 Emission from the three controllers of scenario 4-6 in case 1 are shown in Figure 4.10 and Table 4.4. Comparing controlled cases to no control cases, TTT is more or less the same. Hence, fuel consumption and tailpipe emissions are more or less the same since they are related to travel time given that the Total Distance Traveled (TDT) is a constant. Safety measurements,such as number of stops are reduced from 30% to 60% for scenario 4-6, and number of lane changes are reduced consistently.

The performance measurements, i.e., Total Travel Time (TTT), Average Number of Stops (per car), Average Number of Lane Changes (per car), Average Fuel Consumption, and Average CO_2 Emission from the three controllers of scenario 7-10 in case 2 are shown in Figure 4.11 and Table 4.4. Case 2 is a long accident (1 hour) blocking one of two freeway lanes. These four scenarios (scenario 7-10) are designed to test the effects of controllers at different demand levels, ranging from very heavy to very light traffic. Comparing controlled cases to no control cases, when demand is very heavy and moderate heavy, TTT is more or less the same. However, when demand is light, controllers actually increase travel time. This is consistent with our intuition that when traffic is light enough, the 50% capacity of the bottleneck could handle all the traffic demand, therefore slowing down vehicles unnecessarily increases travel time,fuel consumption and tailpipe emissions. In case 2, Desired Speed Decision points are placed more frequently with smaller speed change intervals, hence vehicles experience smoother speed profiles when controlled. With the same travel time, fuel consumptions and tailpipe emissions are reduced by about 5% when traffic is heavy (scenario 7 and 8). For number of stops, when

demand is moderate heavy, the improvement of controlled cases are the biggest. When traffic is very light, again, controllers actually make vehicles stop a little bit more. In terms of number of lane changes, only when traffic is moderate heavy, controllers could reduce number of lane changes.

4.4.3 Summary of Results

The average (across random seeds) performance measurements of each of the 10 traffic scenarios are tabulated in Table 4.4. The summary conclusions of the results are as follows,

- All the measurements suggest that the simple controller with less computational burden is not inferior to the more complicated model predictive controller (MPC).
- In terms of average number of stops, the simple controller has consistently better improvement over MPC.
- Although macroscopic simulations demonstrates that both simple controller and model predictive controller could reduced Total Time Spent (TTS) for about 20%, VISSIM microscopic simulations show that Total Travel Time (TTT) could not be improved by variable speed limit controllers. Microscopic models capture more detailed vehicle interactions both longitudinally and latitudinally. Vehicles's transient responses to speed controllers are not showing in macroscopic models. Moreover, upstream of the studied freeway segment in macroscopic models is modeled as a virtual parking lot, the effects of second rate shock waves are not included. If looking at the individual vehicle trajectories more closely, one could find that by applying VSL control, some of the vehicles could have shorter travel time but some other vehicles will have longer travel time. On average, the total travel time of the system is not reduced. For example, as shown in Figure 4.12 and Figure 4.13, vehicle

NO. 693 gets to the destination faster by slowing down earlier due to the speed controller but vehicle NO. 1293 has a longer travel time also due to the speed controller.

- Given that the Total Distance Traveled (TDT) is a constant, fuel consumption and tailpipe emissions are similar to TTT. For example, as shown in Figure 4.14, simple controller reduces fuel consumption for vehicle NO.500-1000, but increase it for vehicle NO. 1500-2000. On average, as a system, the fuel consumption is not reduced for most of the scenarios except scenario 7 and 8. The reason why scenario 7 and 8 could show any fuel consumption and tailpipe emission benefits is because the DSD points are placed every 100 meters to force the vehicles to change speed in a smoother way. Therefore, traditional speed limit controller such as those implemented in a overhead message sign manner is not effective in reducing fuel consumption and tailpipe emission. Individual vehicle level speed profile control (such as the one proposed in [5]) could be combined to give environmental benefits. If in the future, VSLs are implemented through roadside to vehicle communication and realized by Adaptive Cruise Control (ACC), some environmental benefits could be achieved.

- One of the safety benefits indicator– number of lane changes are reduced but not by much. Integrating lane change control with speed limit control might give more such benefits.

- The effectiveness of VSL controllers are dependent on the traffic demand level and the congestion level. If the demand is low, VSL controllers could cause unnecessary slowing down (scenario 9 and 10). If the demand is too high and the congestion is too severe, VSL controller are not going to be effective either (scenario 7) because there is no room for improvement. Therefore, the

effective region is at the top of the fundamental diagram close to the critical density ρ_c as shown in Figure 4.15.

Table 4.4: VISSIM Simulations Performance Measurements

Scenario NO.	Ave Demand (veh/h /lane)	Total Number of Vehicles	ctrl	TTS (hours)	%	Ave Speed (km/h)	Ave Number of Stops (per vehicle)	%	Ave Lane Change (per vehicle)	%	Ave Fuel (g/km /veh)	%	Ave CO2 (g/km/ veh)	%
1	1800	11250	No Control	1068.0		95.1	0.52		4.97		76.6		242.6	
			Simple Controller	1095.0	2.5	92.7	0.09	-82.3	4.68	-5.9	78.6	2.6	248.9	2.6
			MPC Controller	1087.5	1.8	93.4	0.16	-70.4	4.59	-7.7	78.9	2.9	249.7	2.9
2	1700	10625	No Control	975.7		98.2	0.26		4.96		73.6		233.2	
			Simple Controller	993.2	1.8	96.5	0.02	-92.7	4.74	-4.4	74.6	1.4	236.4	1.4
			MPC Controller	992.8	1.8	96.5	0.08	-70.2	4.65	-6.1	75.6	2.7	239.6	2.7
3	1800	11250	No Control	1239.8		82.1	2.77		4.71		89.4		283.2	
			Simple Controller	1247.7	0.6	81.5	1.81	-34.8	4.43	-6.0	89.8	0.4	284.3	0.4
			MPC Controller	1309.9	5.7	77.7	2.08	-24.9	4.14	-12.2	92.9	3.9	294.3	3.9
4	1900	8550	No Control	1673.8		87.0	3.20		5.25		85.3		270.3	
			Simple Controller	1675.9	0.1	86.9	1.71	-46.6	5.03	-4.2	85.9	0.6	272.0	0.6
			MPC Controller	1691.0	1.0	86.1	1.88	-41.4	4.97	-5.4	86.2	1.0	273.0	1.0
5	1800	8100	No Control	1489.3		92.6	1.97		5.60		79.6		252.0	
			Simple Controller	1490.4	0.1	92.5	0.75	-62.0	5.42	-3.2	79.8	0.3	252.8	0.3
			MPC Controller	1493.1	0.3	92.4	0.83	-57.6	5.39	-3.7	79.6	0.1	252.2	0.1
6	1900	8550	No Control	1759.1		82.8	4.54		5.13		89.6		283.8	
			Simple Controller	1755.4	-0.2	83.0	2.89	-36.3	4.91	-4.2	89.9	0.4	284.8	0.4
			MPC Controller	1767.0	0.4	82.4	2.96	-34.8	4.87	-5.0	89.8	0.2	284.4	0.2
7	1200	4800	No Control	1740.1		47.5	34.33		0.87		184.0		583.0	
			Simple Controller	1739.2	-0.1	47.6	31.79	-7.4	0.92	6.0	173.6	-5.7	550.0	-5.7
			MPC Controller	1746.6	0.4	47.3	32.76	-4.6	0.90	3.7	176.5	-4.1	559.0	-4.1
8	1000	4000	No Control	1051.1		65.7	16.66		0.76		146.2		463.0	
			Simple Controller	1053.3	0.2	65.6	12.80	-23.2	0.74	-3.1	139.5	-4.6	441.9	-4.6
			MPC Controller	1050.1	-0.1	65.7	13.92	-16.5	0.75	-1.6	139.1	-4.9	440.5	-4.9
9	750	3000	No Control	522.2		97.9	1.43		0.73		72.6		230.0	
			Simple Controller	562.6	7.7	90.9	0.67	-53.1	0.86	17.1	77.9	7.3	246.8	7.3
			MPC Controller	531.0	1.7	96.2	1.30	-9.0	0.84	15.0	73.4	1.1	232.5	1.1
10	500	2000	No Control	323.7		105.1	0.00		0.26		68.6		217.2	
			Simple Controller	353.7	9.3	96.3	0.01		0.45	70.2	74.4	8.5	235.7	8.5
			MPC Controller	333.9	3.1	101.9	0.01		0.45	71.7	70.8	3.2	224.3	3.2

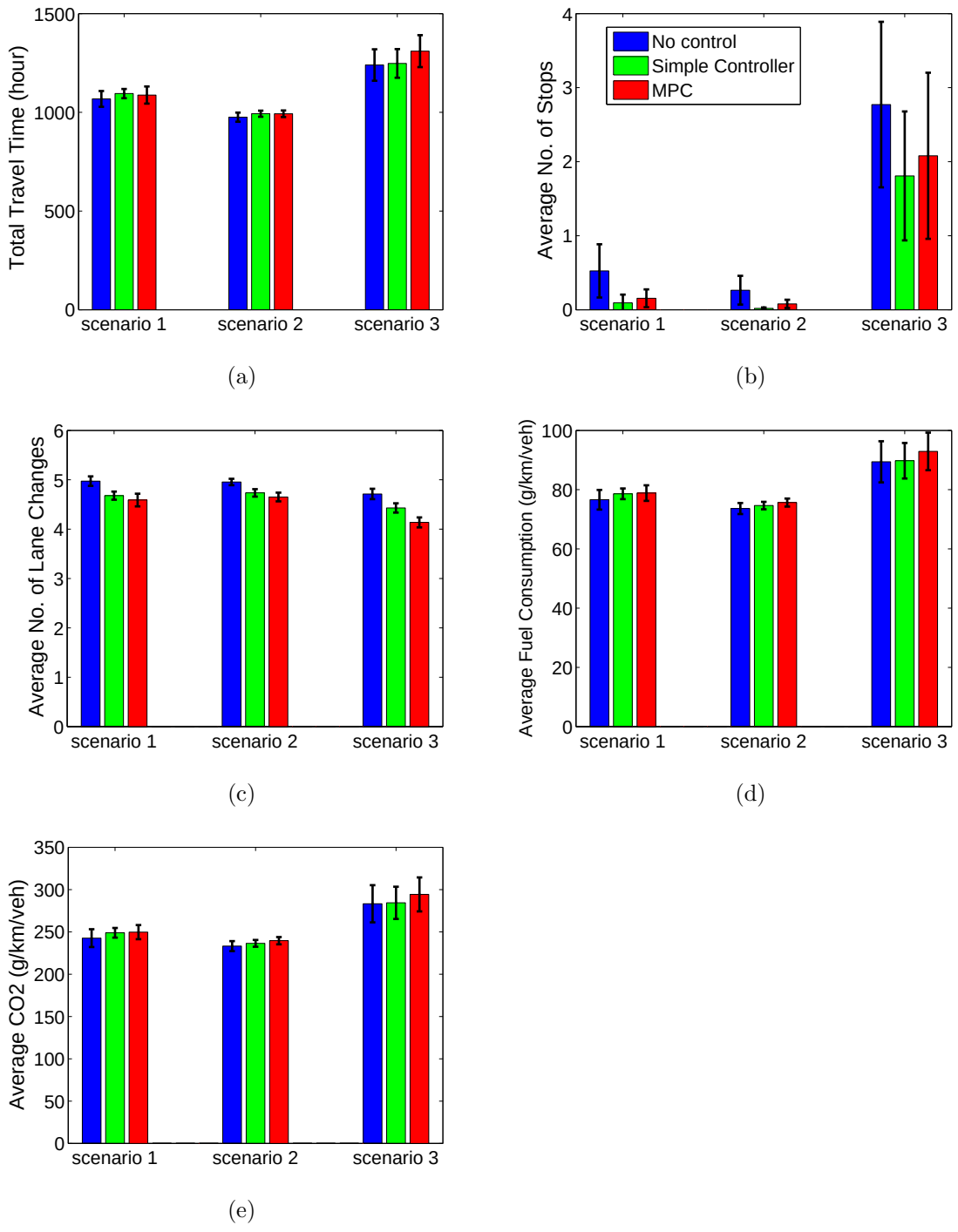

Figure 4.9: Network II: (a) Total Travel Time (b) Average Number of Stops, (c) Average Number of Lane Changes , (d) Average Fuel Consumption, (e) Average CO_2 Emission.

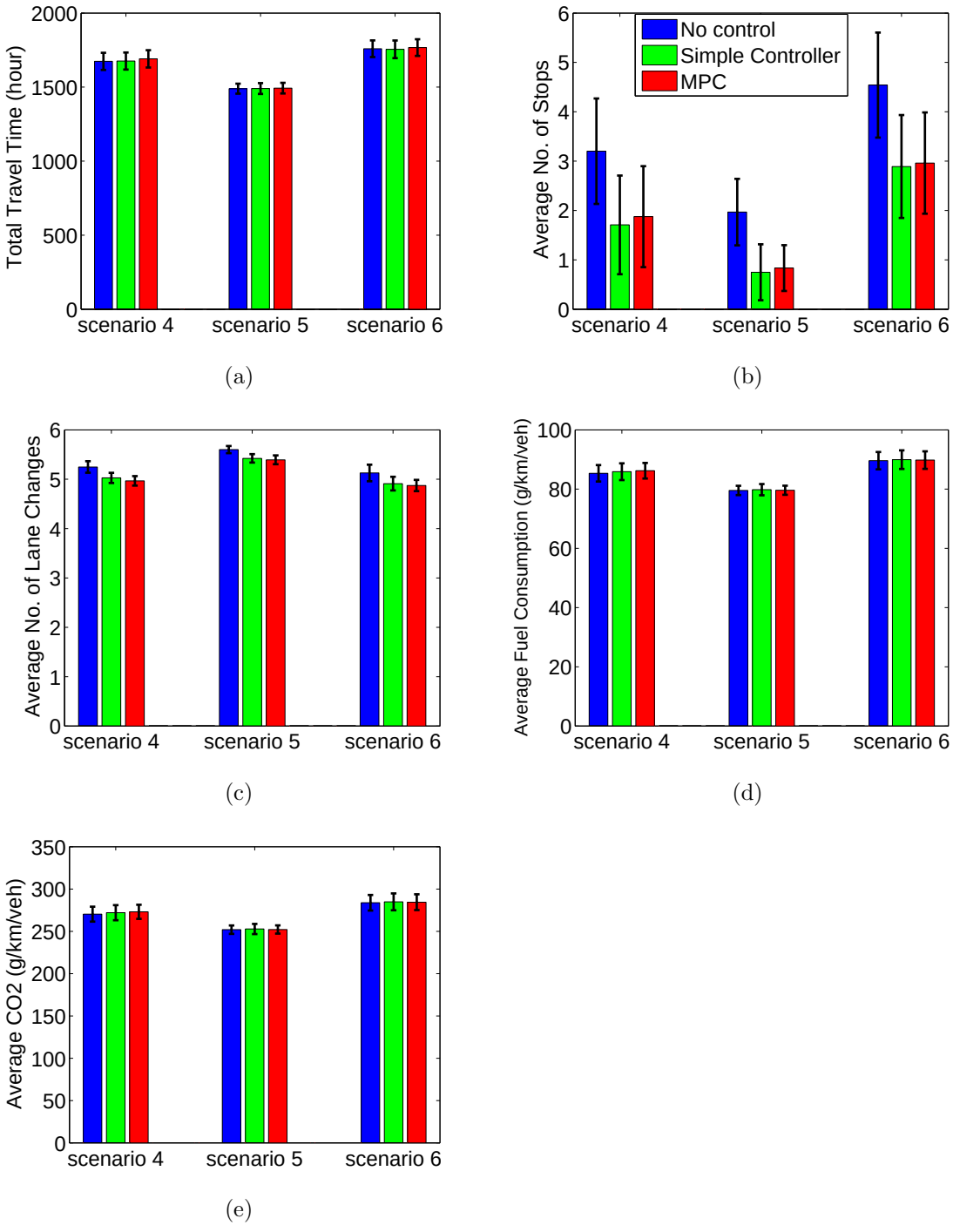

Figure 4.10: Network III Case 1: (a) Total Travel Time (b) Average Number of Stops, (c) Average Number of Lane Changes , (d) Average Fuel Consumption,(e) Average CO_2 Emission.

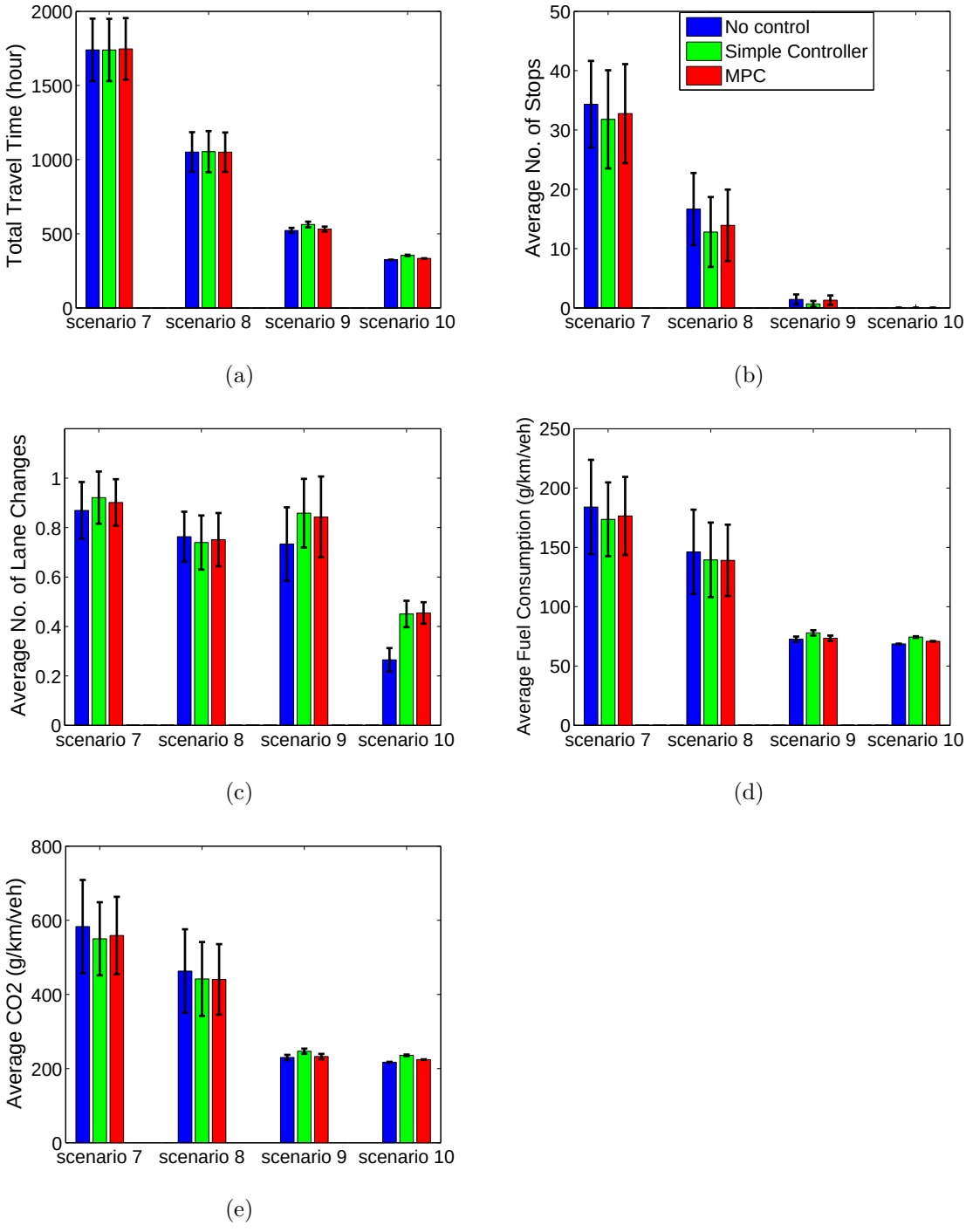

Figure 4.11: Network III Case 2: (a) Total Travel Time (b) Average Number of Stops, (c) Average Number of Lane Changes , (d) Average Fuel Consumption, (e) Average CO_2 Emission.

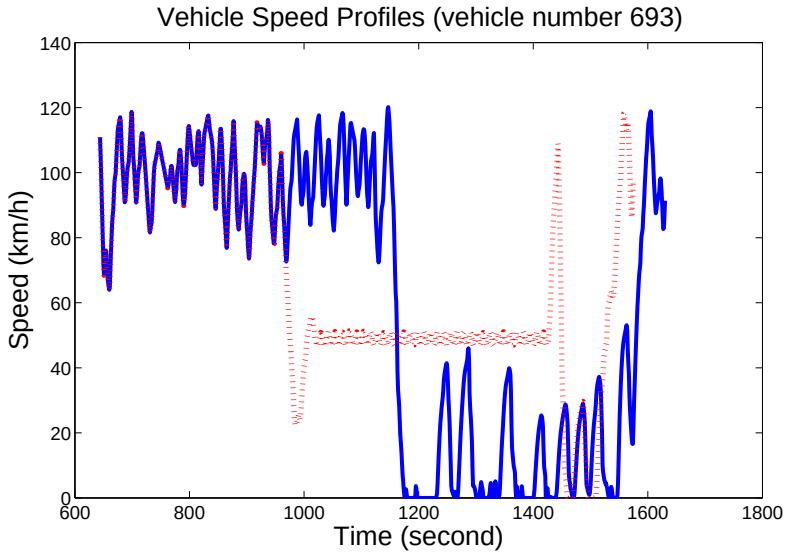

(a)

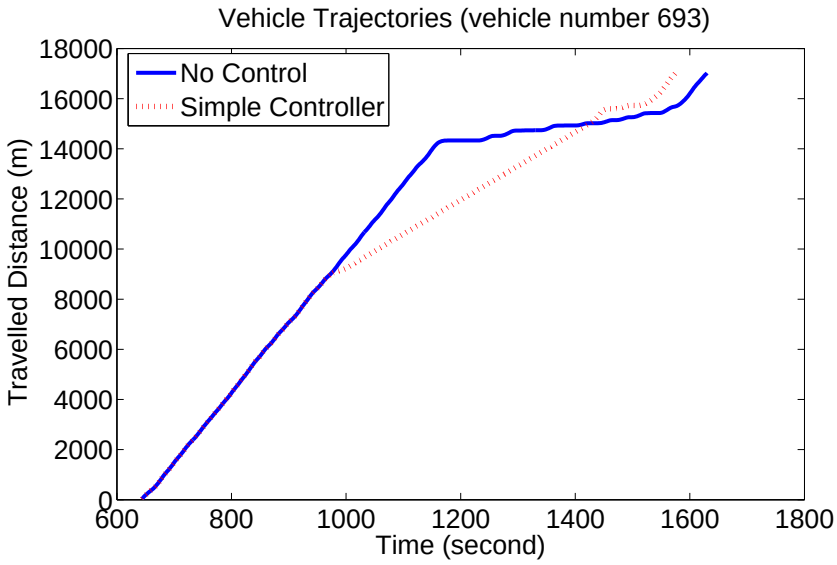

(b)

Figure 4.12: Vehicle No. 693 speed profile and trajectory : (a) Speed Profile, (b) Trajectory.

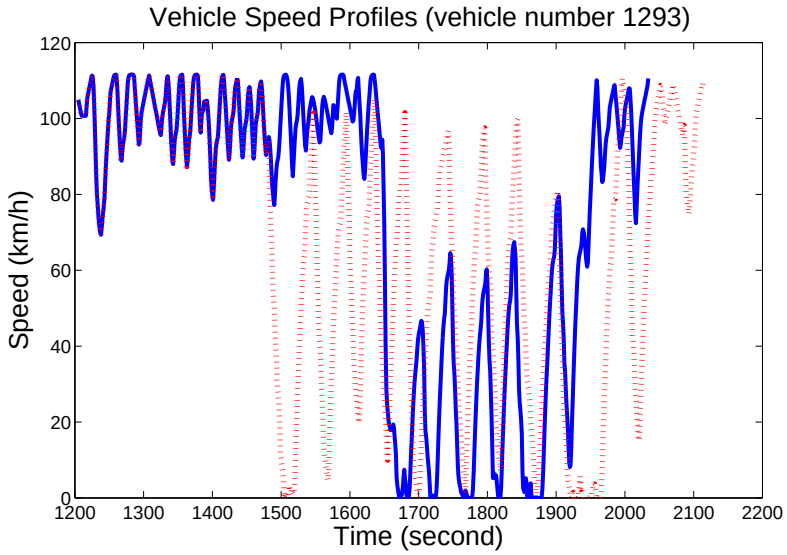

(a)

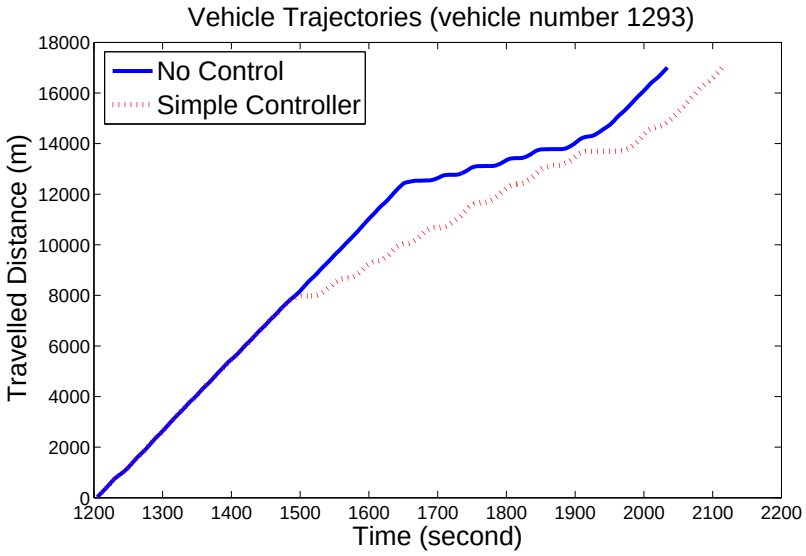

(b)

Figure 4.13: Vehicle No. 1293 speed profile and trajectory: (a) Speed Profile, (b) Trajectory.

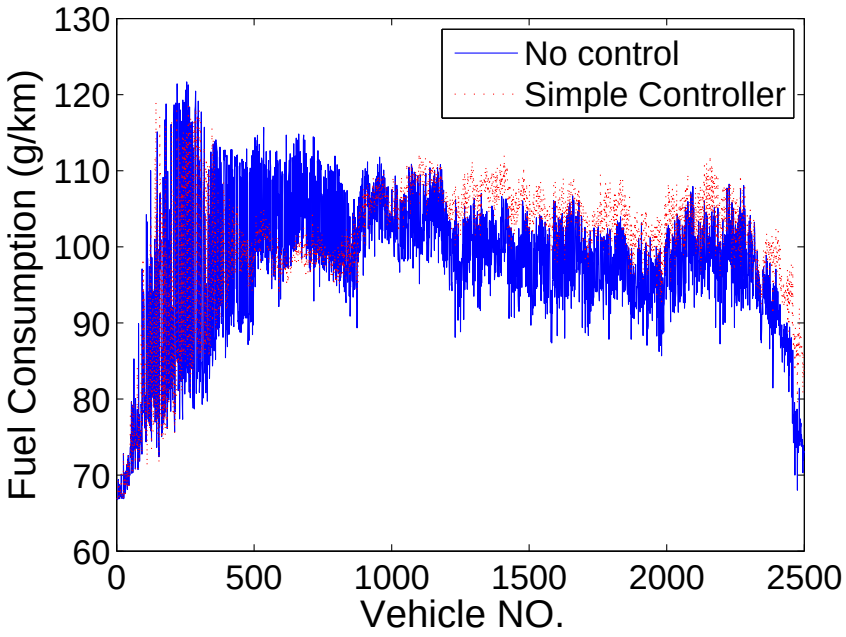

Figure 4.14: Fuel Consumption Comparison

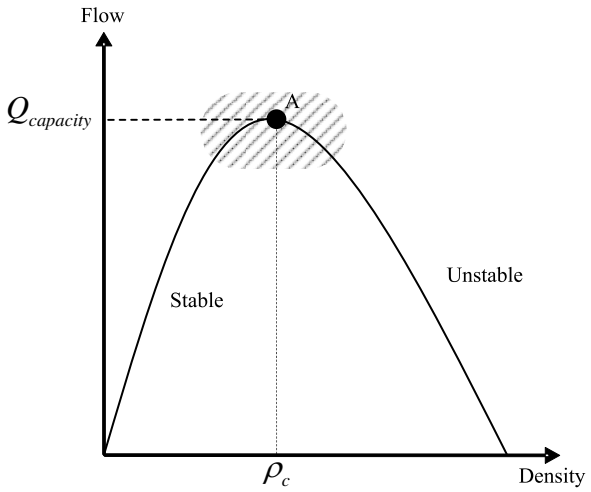

Figure 4.15: Effective Region in Fundamental Diagram (shown as shaded area)

Chapter 5

Conclusions

In this study, a control engineering approach is applied to design, analyze and evaluate variable speed limit controllers. Two types of speed controllers, simple PI type controllers and model predictive controllers are designed and analyzed using macroscopic (PDE) models, and their performance in terms of mobility, safety and environmental benefits are evaluated using the stochastic and more realistic microscopic traffic flow simulator VISSIM.

- The original macroscopic flow model (LWR model) developed from fluid dynamics doesn't have the VSL module. All the existing macroscopic models for incorporating effects of VSL are based on modifications of the steady state fundamental diagram. A new VSL model is developed in this study from driver behaviors. The proposed model is validated using simulated data of microscopic models (VISSIM) and is compared to an existing macroscopic model modified to account for VSL. It is shown that the proposed model has more accurate descriptions of the transient effects of VSL than the existing model which has only take into account the steady state effects of speed control inputs.

- A PI type virtual mainline metering VSL controller is designed based on the fundamental flow-density relationship and analyzed using the macroscopic model.

- A Nonlinear model predictive VSL controller with consideration of environmental benefits in the cost function is proposed and evaluated using the macroscopic model.
- A proportional VSL that only takes density measurements as inputs is designed and shown by macroscopic simulations to be non inferior to the model predictive controller in [13] which gave a TTS improvement up to 20%.
- An open loop lane change controller is designed using VISSIM for traffic accident scenarios.
- An integrated simulation/evaluation framework with VISSIM, VISSIM COM interface, a C++ program and MATLAB APIs to realize the feedback control system. Online traffic state measurements such as link speeds and densities are obtained from VISSIM COM interface and sent to controllers implemented in MATLAB. Speed commands generated by MATLAB code are sent to VISSIM COM interface to control traffic in real time.
- Integrated the CMEM emission model with VISSIM so that the environmental benefits of VSL control could be analyzed.
- The robustness question of the VSL controllers, that is to what extent VSL control could be beneficial for both mobility and environment, is studied through simulation runs with 10 different traffic scenarios with different freeway geometry, demand levels, bottleneck scenarios, and VSL implementations.
- Considering the stochastic nature of traffic, Monte Carlo simulations for each scenario/case are conducted to test the robustness of VSL control. Performance measurements are compared and analyzed.
  - All the measurements suggest that the simple controller with less computational burden is not inferior to the more complicated nonlinear MPC.

- Although macroscopic simulations demonstrates that both simple controller and model predictive controller could reduced Total Time Spent (TTS) for about 20%, VISSIM microscopic simulations show that Total Travel Time (TTT) could not be improved by variable speed limit controllers.
- Safety benefits of VSL controllers such as reducing number of stops and reducing number of lane changes are demonstrated through VISSIM simulations.
- If the VSL controllers are implemented in a overhead message sign manner spaced every few hundreds meters to 1 kilometer, environmental benefits is hard to achieve by VSL control along. Vehicle level speed profile shaping is needed to smooth vehicle acceleration/deceleration trajectories to obtain fuel savings and reduce tailpipe emissions.
- The effectiveness of VSL controllers are dependent on the traffic demand level and the congestion level. VSL controllers are more effective when traffic density is close to the critical density and would not be effective when traffic density is too high. It will have negative benefits when traffic density is so low that speed control causes unnecessary slowing down of the traffic flow.

While both VSL control and open loop lane change control are shown to have safety benefits, it would be interesting to integrate VSL control with feedback lane change control.

Reference List

[1] Available at http://www.caradvice.com.au/27779/uk-speed-limit-petition-gathers-pace/.

[2] A. Alessandri, A. Di Febbraro, A. Ferrara, and E Punta. Nonlinear optimization for freeway control using variable-speed signaling. *IEEE Transactions on Vehicular Technology*, 48(6):2042–2052, 1999.

[3] P. Allaby, B. Hellinga, and M. Bullock. Variable speed limits: Safety and operational impacts of a candidate control strategy for freeway applications. *IEEE Transactions on Intelligent Transportation Systems*, 8(4):671–680, 2007.

[4] F. An, M. Barth, J. Norbeck, and M. Ross. Development of comprehensive modal emissions model operating under hot-stabilized conditions. *Transportation Research Record*, 1587:52–62, 1997.

[5] M. Barth and K. boriboonsomsin. Energy and emissions impacts of a freeway-based dynamic eco-driving system. *Transportation Research Part D*, 14:400–410, 2009.

[6] R. C. Carlson, I. Papamichail, M. Papageorgiou, and A. Messmer. Optimal mainstream traffic flow control of large-scale motorway networks. *Transportation Research Part C*, 18(2):193–212, 2010.

[7] H. Chang, Y. Wang, J. Zhang, and P. A. Ioannou. An integrated roadway controller and its evaluation by microscopic simulator vissim. In *Proceedings of European Control Conference*, pages 2436–2441, Kos,Greece, July 2007.

[8] Y. Chiang and J. Juang. Control of freeway traffic flow in unstable phase by h-infinity theory. *IEEE Transactions on Intelligent Transportation Systems*, 9(2):193–208, 2008.

[9] M. Cremer. A new scheme for traffic flow estimation and control. In *Proceedings of 3rd IFAC/IFIP/IFORS Symposium*, pages 29–37, Columbus,OH, 1976.

[10] M. Cremer and S. Schoof. On control strategies for urban traffic corridors. In J. P. Perrin, editor, *Control, Computers, Communications in Transportation,*

Selected Papers from the IFAC/IFIP/IFORS Symposium, Paris, France, 19-21 September 1989, pages 213–219. Pergamon Press, 1990.

[11] C. F. Daganzo. The cell transmission model: A dynamic representation of highway traffic consistent with the hydrodynamic theory. *Transportation Research Part B*, 28(4):269–287, 1994.

[12] A. Di Febbraro, T. Parisini, S. Sacone, and R. Zoppoli. Neural approximation for feedback optimal control of freeway systems. *IEEE Transactions on Vehicular Technology*, 50(1):302–313, 2001.

[13] A. Hegyi, B. De Schutter, and J. Hellendoorn. Optimal coordination of variable speed limits to suppress shock waves. *IEEE Transactions on Intelligent Transportation Systems*, 6(1):102–112, 2005.

[14] A. Hegyi, B. De Shutter, and H. Hellendoorn. Model predictive control for optimal coordination of ramp metering and variable speed limits. *Transportation Research Part C*, 13:185–209, 2005.

[15] E. Van De Hoogen and S. Smulders. Control by variable speed signs: Results of the dutch experiment. *Proc. Road Traffic Monit. Control IEE Conf. Pub.*, 391:145–149, 1994.

[16] M. Jha, D. Cuneo, and M. Ben-Akiva. Evaluation of freeway lane control for incident management. *Journal of Transportation Engineering*, 125:495–501, 1999.

[17] B. Kamel, A. Benasser, and D. Jolly. Flatness based control of traffic flow for coordination of ramp metering and variable speed limits. In *International IEEE Conference on Intelligent Transportation Systems*, pages 838–843, Beijing,China, October 2008.

[18] U. Karaaslan, P. Varaiya, and J. Walrand. Two proposals to improve freeway traffic flow. In *Proc. American Control Conf.*, Boston,MA,USA, 1991.

[19] J. A. Laval and C. F. Daganzo. Lane-changing in traffic streams. *Transportation Research Part B*, 40:251–264, 2006.

[20] M. J. Lighthill and G. B. Whitham. On kinematic waves ii: A theory of traffic flow on long crowded roads. *Proceedings of the Royal Society of London. Series A, Mathematical and Physical Sciences*, 229(1178):317–345, 1955.

[21] X. Lu, P. varaiya, R. Horowitz, D. Su, and S. E. Shladover. A new approach for combined freeway variable speed limits and coordinated ramp metering. In *International IEEE Conference on Intelligent Transportation Systems*, pages 491–498, Madeira Island, Portugal, September 2010.

[22] X. Y. Lu, P. Varaiya, and R. Horowitz. An equivalent second order model with application to traffic control. In *Proceedings of the 12th IFAC Symposium on Transportation Systems*, pages 375–382, Redondo Beach,California, September 2009.

[23] H. S. Mahmassani and R. Jayakrishnan. Dynamic analysis of lane closure strategies. *Journal of Transportation Engineering*, 114:476–496, 1988.

[24] M. Menendez and C. F. Daganzo. Effects of hov lanes on freeway bottlenecks. *Transportation Research Part B*, 41(8):809–822, 2007.

[25] A. Messmer and M. Papageorgiou. Metanet: a macroscopic simulation program for motorway network. *Traffic Engineering and Control*, 31(8):466–470, 1990.

[26] J. Oh and C. Oh. Dynamic speed control strategy for freeway traffic congestion management. *Journal of the Eastern Asia Society for Transportation Studies*, 6:595–607, 2005.

[27] M. Papageorgiou, J. Blosseville, and H. Hadj-Salem. Macroscopic modelling of traffic flow on the boulevard peripherique in paris. *Transportation Research Part B*, 23(1):29–47, 1989.

[28] M. Papageorgiou, H. Hadj-Salem, and F. Middelham. Alinea local ramp metering: summary of field results. *Transportation Research Record*, 1603:90–98, 1997.

[29] M. Papageorgiou, E. Kosmatopoulos, and I. Papmichail. Effects of variable speed limits on motorway traffic flow. *Transportation Research Record*, 2047:37–48, 2008.

[30] M. Papageorgiou, I. Papamichail, A. D. Spiliopoulou, and A. F. Lentzakis. Real-time merging traffic control with applications to toll plaza and work zone management. *Transportation Research Part C*, 16:535–553, 2008.

[31] H. J. Payne. Models of freeway traffic and control. *Simulation Council Proceedings, Mathematics of Public Systems*, 1(1):51–61, 1971.

[32] A. Popov, A. Hegyi, R. Babuska, and H. Werner. Distributed controller design approach to dynamic speed limit control against shockwaves on freeways. *Transportation Research Record*, 2086:93–99, 2008.

[33] A. K. Rathi and Z. A. Nemeth. Freesim: A microscopic simulation model of freeway lane closures. *Transportation Research Record*, 1091:21–24, 1986.

[34] P. I. Richards. Shockwaves on the highways. *Operations Research*, 4(1):42–51, 1956.

[35] M. Robinson. Examples of variable speed limit applications. In *Speed Management Workshop Notes, 79th Annual Meeting of Transportation Research Board*, Washington,DC, January 2000.

[36] L. Schaefer, J. Upchurch, and S. A. Ashur. An evaluation of freeway lane control signing using computer simulation. *Mathl. Comput. Modelling*, 27:177–187, 1998.

[37] O. Servin, K. Boriboonsomsin, and M. Barth. A preliminary design of speed control strategies in dynamic intelligent speed adaptation system for freeways. In *Proceedings of the 87th Transportation Research Board Annual Meeting*, Washington,DC, January 2008.

[38] S. A. Smulders. Control of freeway traffic by variable speed signs. *Transportation Research Part B*, 24(2):111–132, 1990.

[39] Y. Wang, H. Chang, and P. Ioannou. Integrated Roadway / Adaptive Cruise Control System: Safety, Performance, Environmental and Near Term Deployment Considerations. Technical Report UCB-ITS-PRR-2007-8, California Partners for Advanced Transit and Highways (PATH), 2007.

[40] Y. Wang, D. Foster, and B. Coifman. Measuring wave speeds on highways during congestion using cross spectral analysis. In *Proceedings of the 7th International IEEE Conference on Intelligent Transportation Systems*, pages 544–547, Washington DC,USA, October 2004.

[41] R. Wiedemann. Simulations des strabenverkehrsflusses. *Schriftenreihe des Instituts für Verkehrswesen der Universität Karlsruhe, Heft 8*, 1974.

[42] R. Wiedemann. Modeling of rti-elements on multi-lane roads. XIII, 1991.

[43] H. Zacker. Beurteilung verkehrsanbhängiger geschwindigkeitsbeschränkungen auf autobahnen. *Straßenbau und Verkehrstchnik, Heft 128*, 1972.

[44] S. Kidane Zegeye, B. De Schutter, H. Hellendoorn, and E. Breunesse. Reduction of travel times and traffic emissions using model predictive control. In *Proc. American Control Conf.*, pages 5393–5397, St. Louis, MO, USA, June 2009.